Improvements in Oscillator Strengths and their Impact on Interstellar Abundances and Depletions

Adam M. Ritchey

ASOS14 – Paris, July 11, 2023

The University of Toledo

Eureka Scientific

Measuring Interstellar Abundances

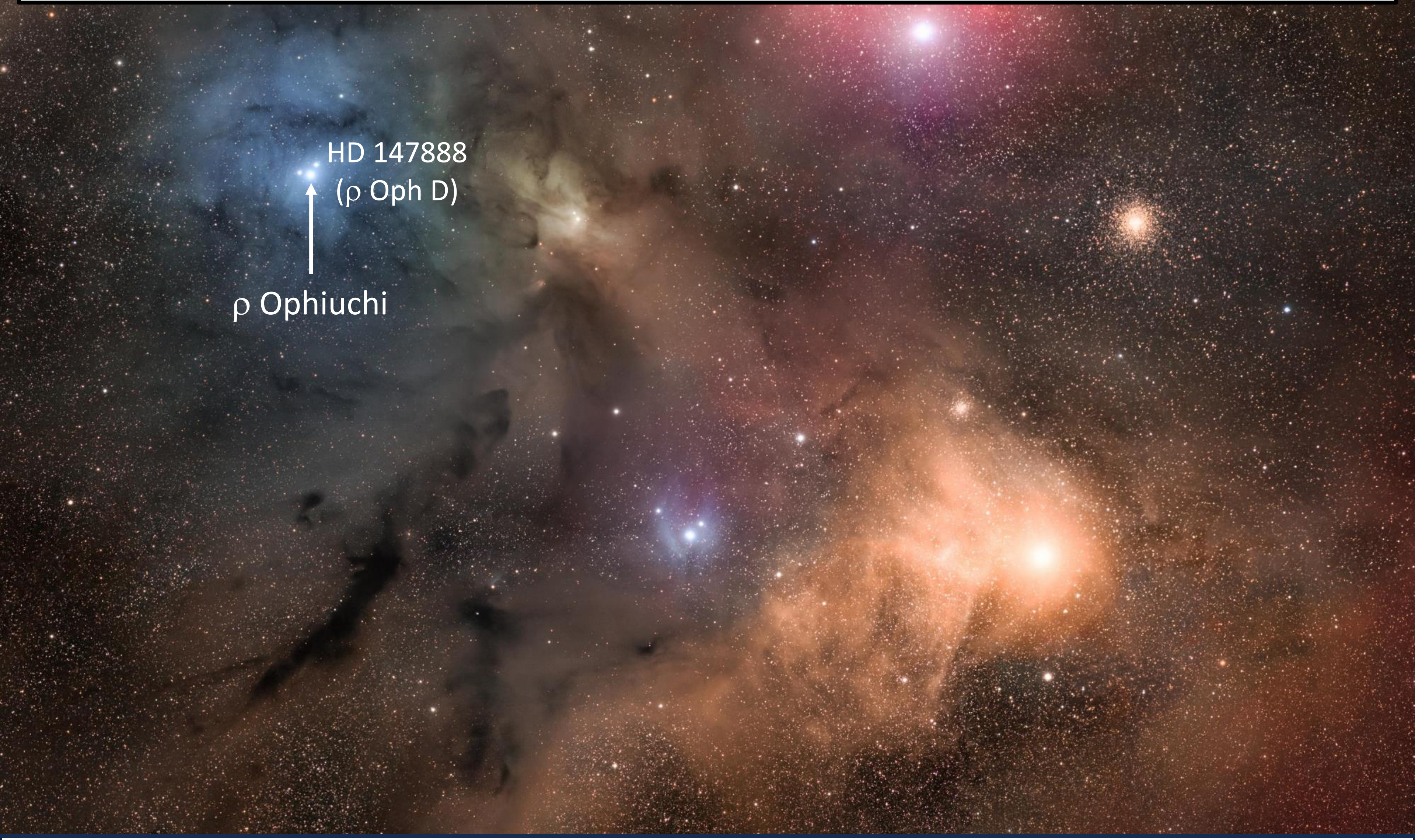

ASOS14 – Paris, July 11, 2023

Adam M. Ritchey

Measuring Interstellar Abundances

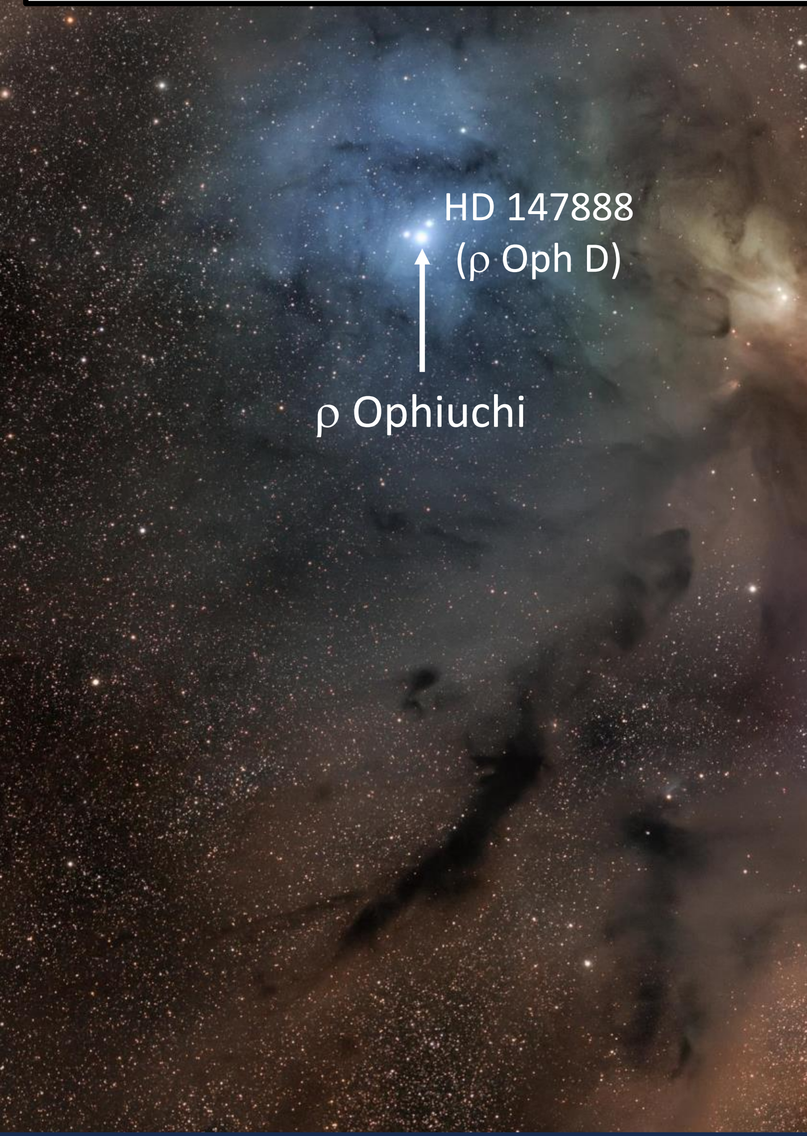

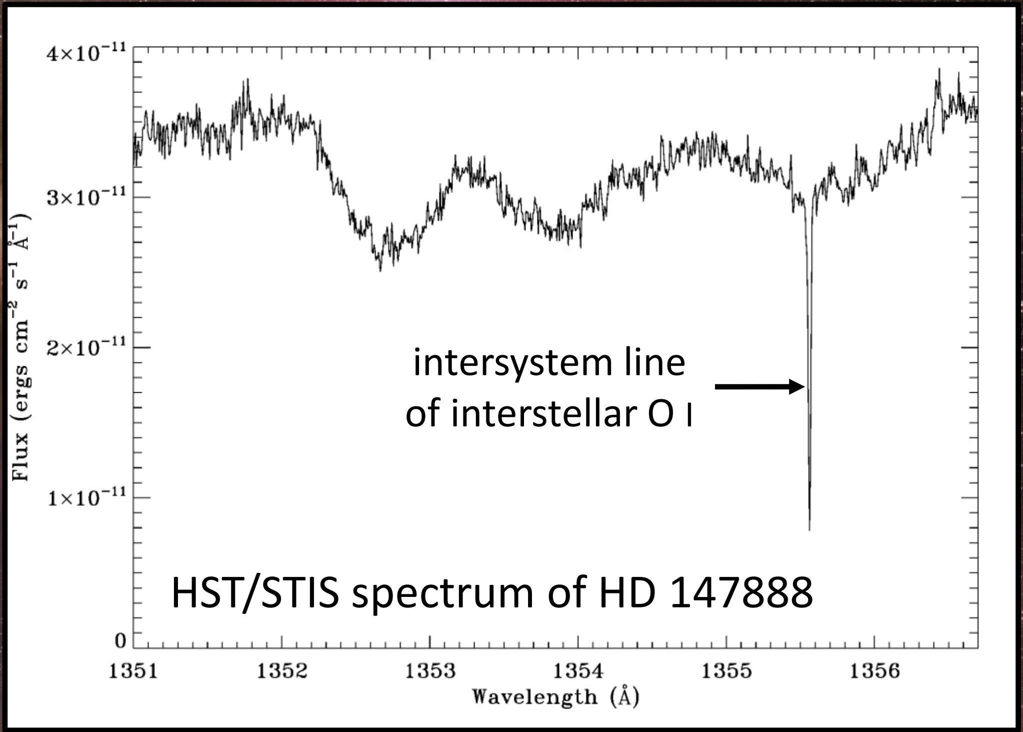

Measuring Interstellar Abundances

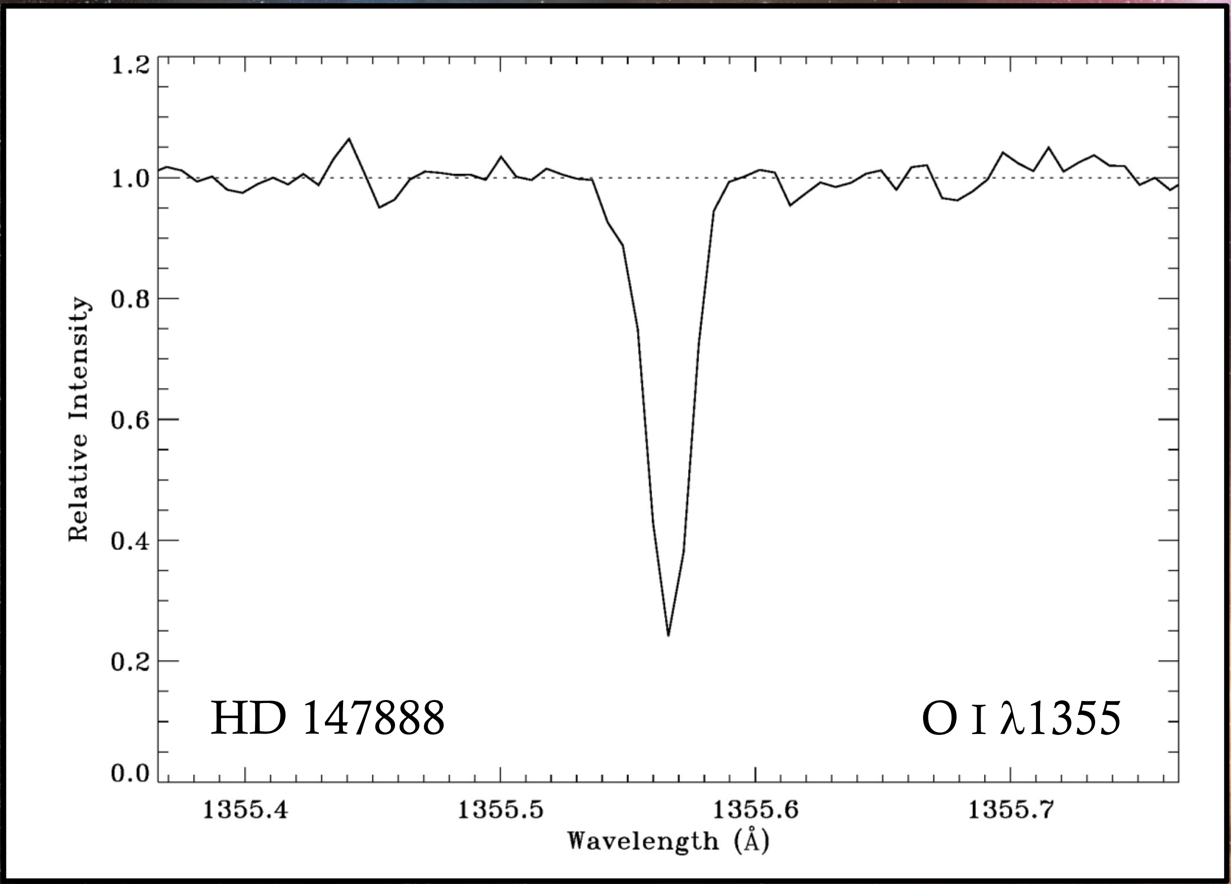

Measuring Interstellar Abundances

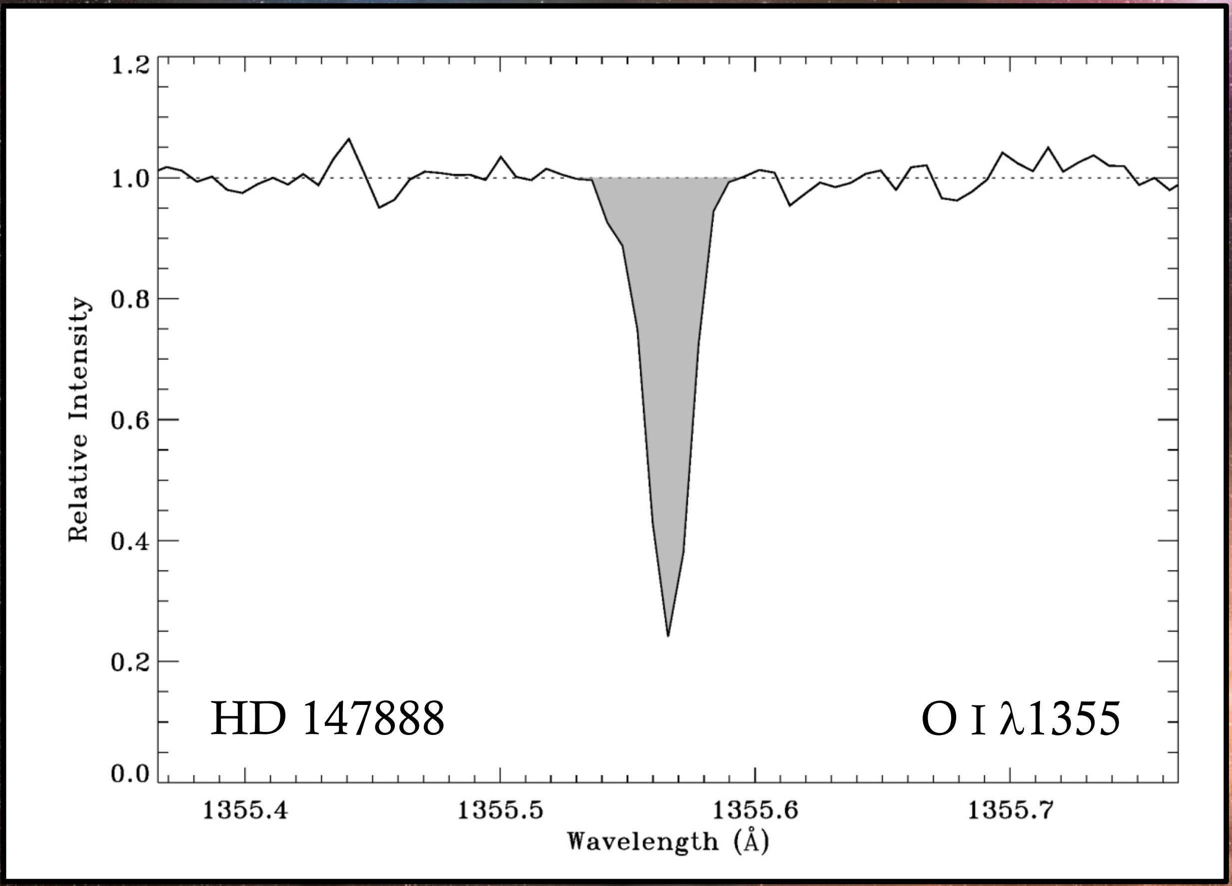

Measuring Interstellar Abundances

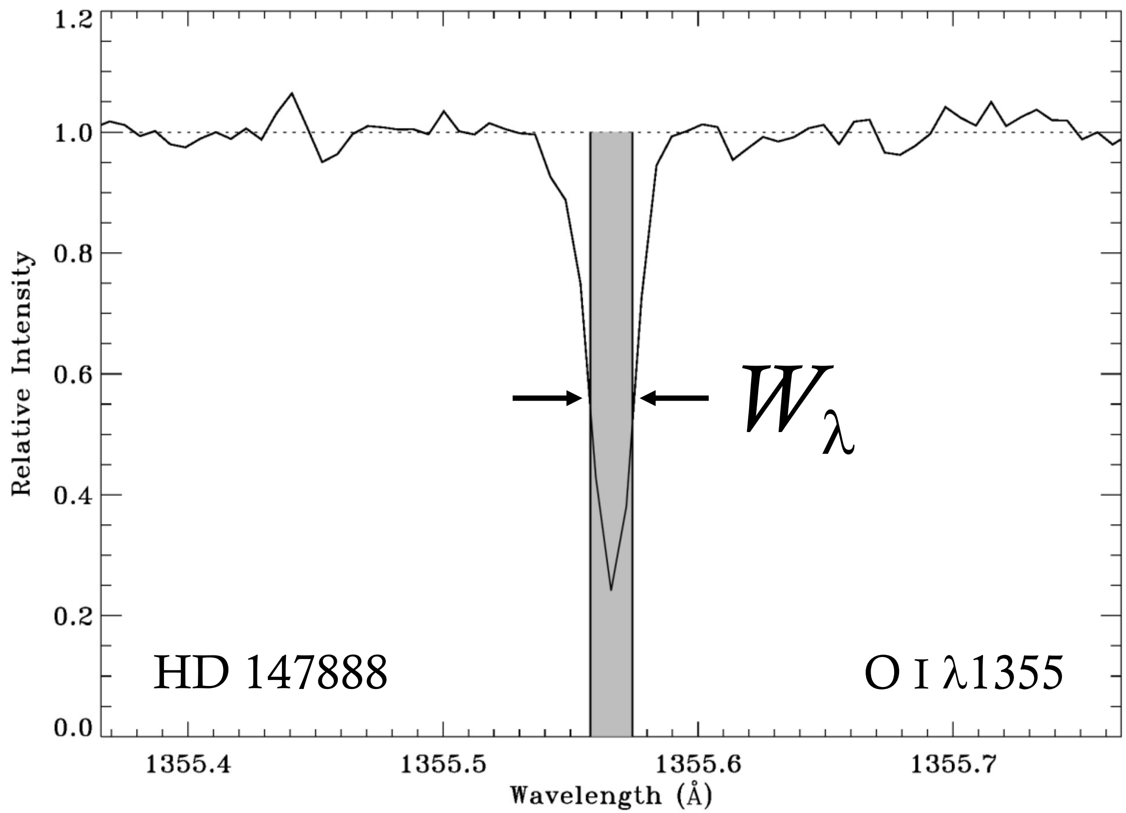

For optically thin absorption:

$$W_\lambda = \frac{\pi e^2}{m_e c^2} N \lambda^2 f$$

W_λ: equivalent width
N: column density
λ: transition wavelength
f: oscillator strength

Measuring Interstellar Abundances

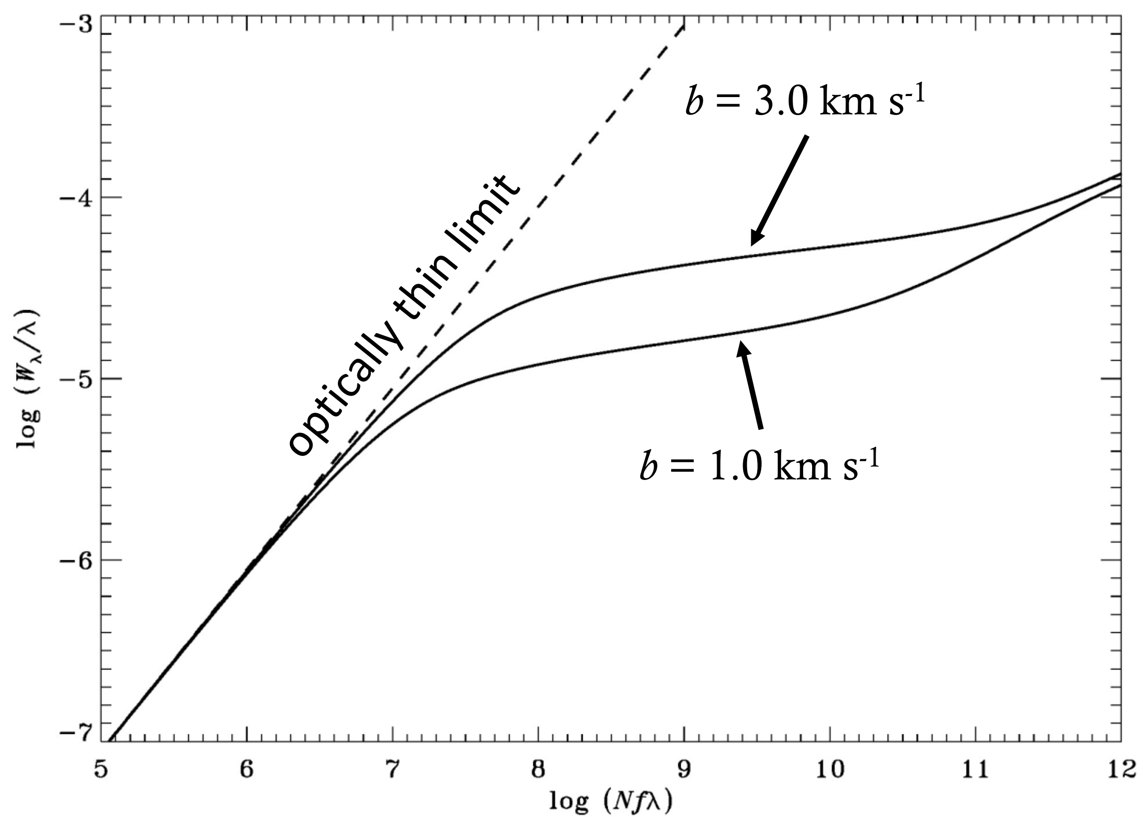

For optically thick absorption, the equivalent width varies as a function of the column density according to a "curve of growth."

Modelling Dust Depletion Trends

For species that represent the dominant ionization stage of their element in neutral diffuse clouds (i.e., I.P. > 13.6 eV), we define the gas-phase elemental abundance:

$$\log (X/\mathrm{H}) = \log N(X) - \log N(\mathrm{H_{tot}}).$$

The "depletion" is then determined by comparing the abundance to a cosmic standard (e.g., the Sun or local B stars):

$$[X/\mathrm{H}] = \log (X/\mathrm{H}) - \log (X/\mathrm{H})_{\odot}.$$

The "missing" atoms are presumed to be locked up in interstellar dust grains.

Modelling Dust Depletion Trends

Element depletion behaviors are modelled adopting the parameterization of Jenkins (2009):

$$[X/\mathrm{H}] = B_X + A_X(F_* - z_X).$$

A_X: depletion "slope"
B_X: depletion at $F_* = z_X$
F_*: sight-line depletion factor

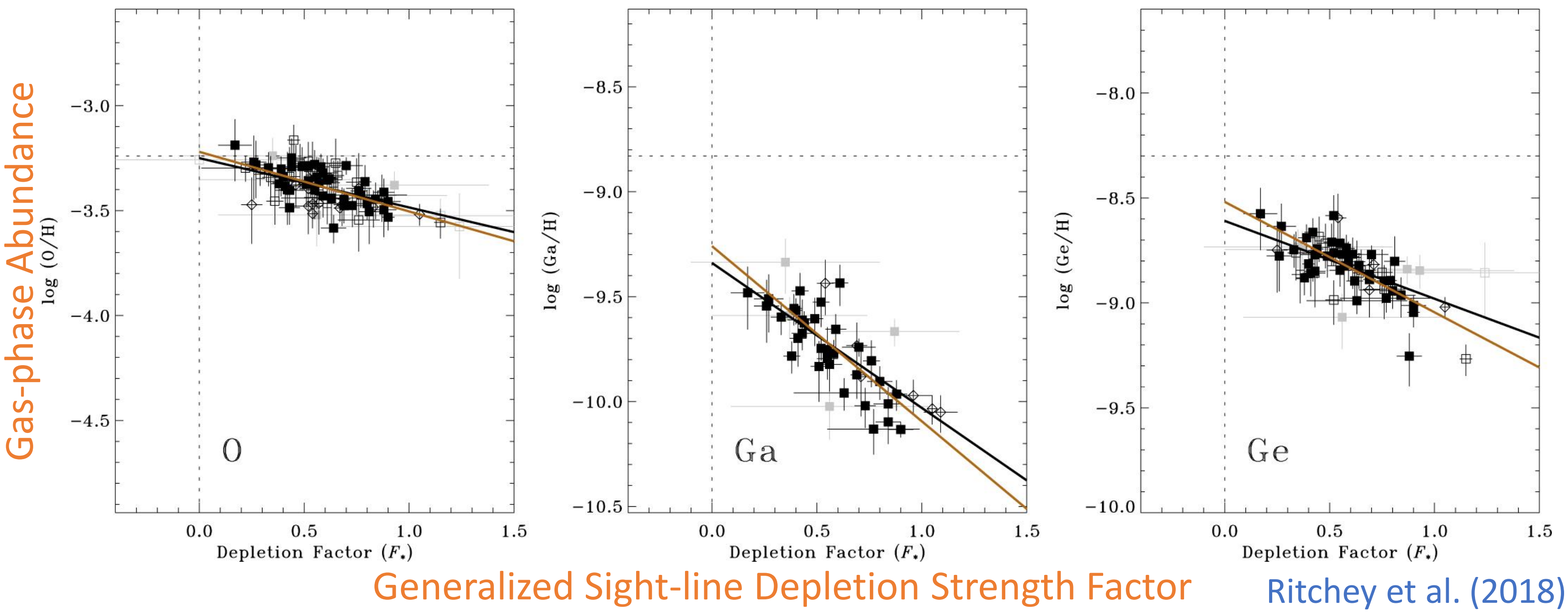

Ritchey et al. (2018)

Modelling Dust Depletion Trends

Element depletion behaviors are modelled adopting the parameterization of Jenkins (2009):

$$[X/\mathrm{H}] = B_X + A_X(F_* - z_X).$$

A_X: depletion "slope"
B_X: depletion at $F_* = z_X$
F_*: sight-line depletion factor

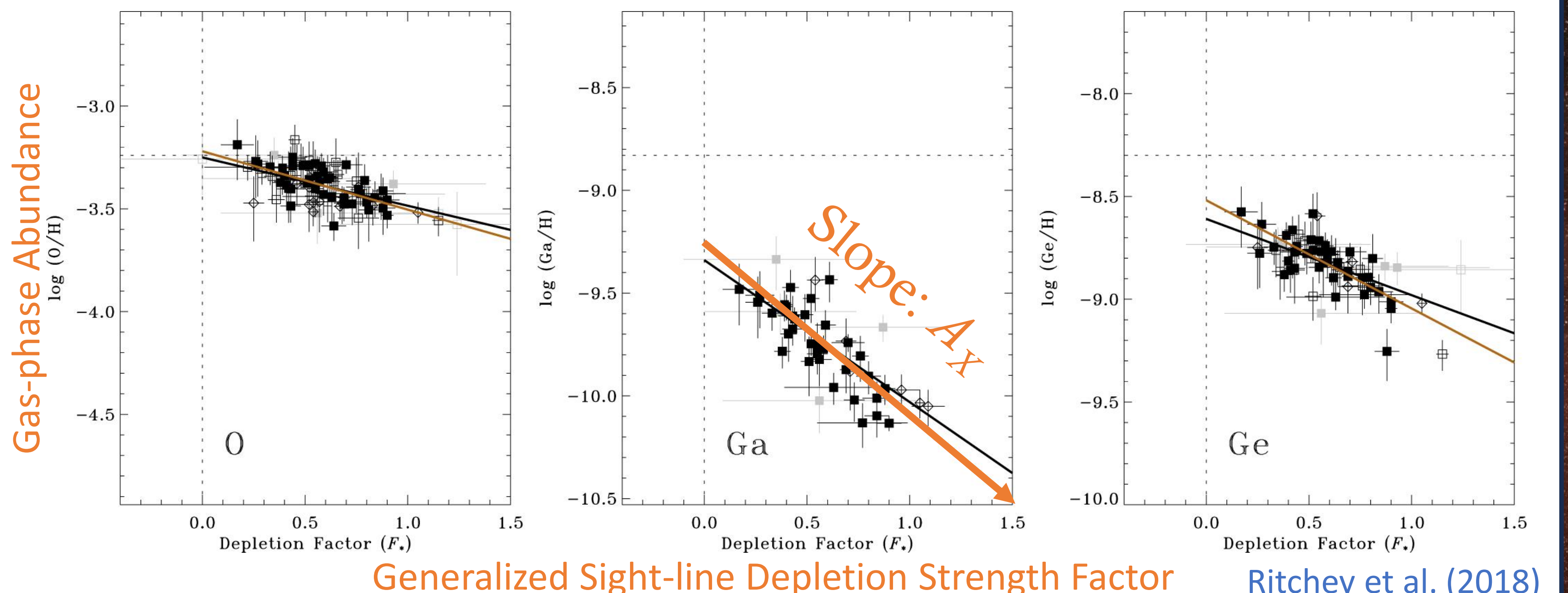

Ritchey et al. (2018)

Modelling Dust Depletion Trends

Element depletion behaviors are modelled adopting the parameterization of Jenkins (2009):

$$[X/\mathrm{H}] = B_X + A_X(F_* - z_X).$$

A_X: depletion "slope"
B_X: depletion at $F_* = z_X$
F_*: sight-line depletion factor

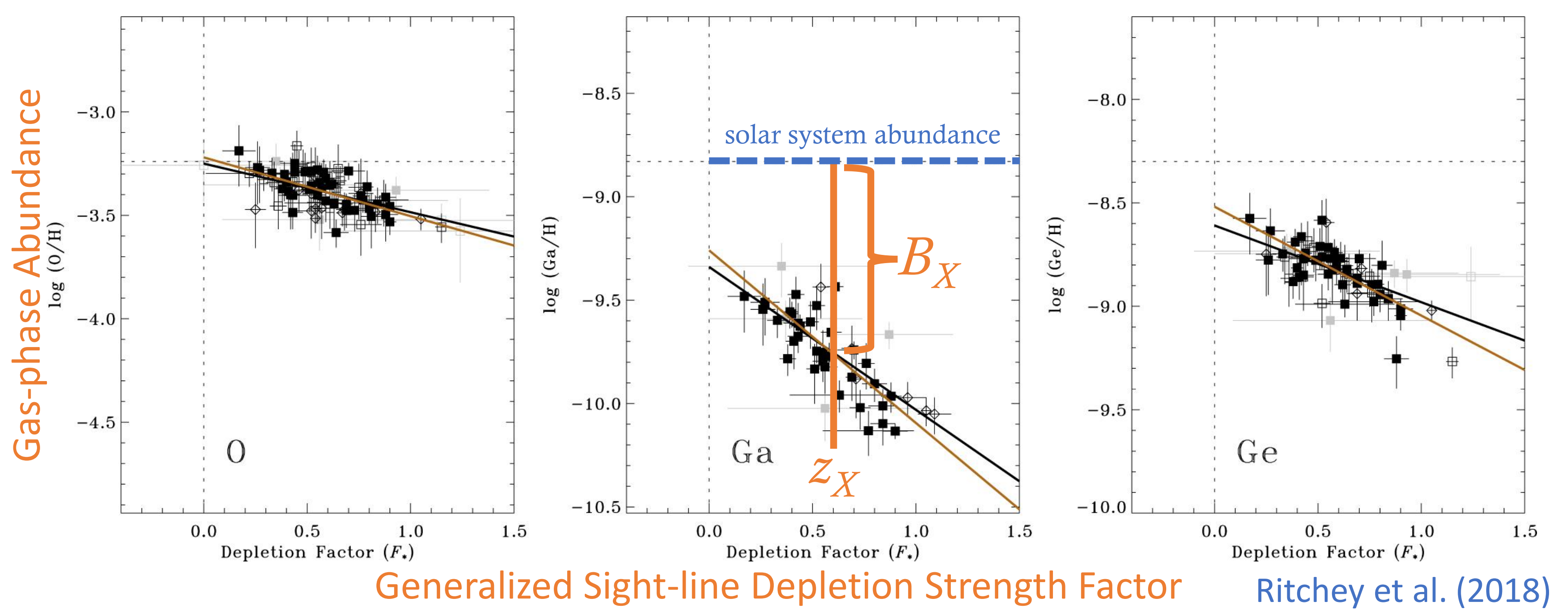

Improvements in Oscillator Strengths

Beam-foil experiments with the Toledo Heavy Ion Accelerator (THIA):

- 330 kV electrostatic positive ion accelerator
- Danfysik Model 911A Universal Ion Source
- Magnetically-selected ions are accelerated and steered toward thin carbon foils with thicknesses of 2.1 to 2.5 μg cm^{-2}.
- Emission lines are analyzed with an Acton 1 m normal incidence vacuum ultraviolet monochromator

Panoramic View of the Toledo Heavy Ion Accelerator:

Improvements in Oscillator Strengths

Beam-foil experiments with the Toledo Heavy Ion Accelerator (THIA):

- 330 kV electrostatic positive ion accelerator
- Danfysik Model 911A Universal Ion Source
- Magnetically-selected ions are accelerated and steered toward thin carbon foils with thicknesses of 2.1 to 2.5 μg cm^{-2}.
- Emission lines are analyzed with an Acton 1 m normal incidence vacuum ultraviolet monochromator

Panoramic View of the Toledo Heavy Ion Accelerator:

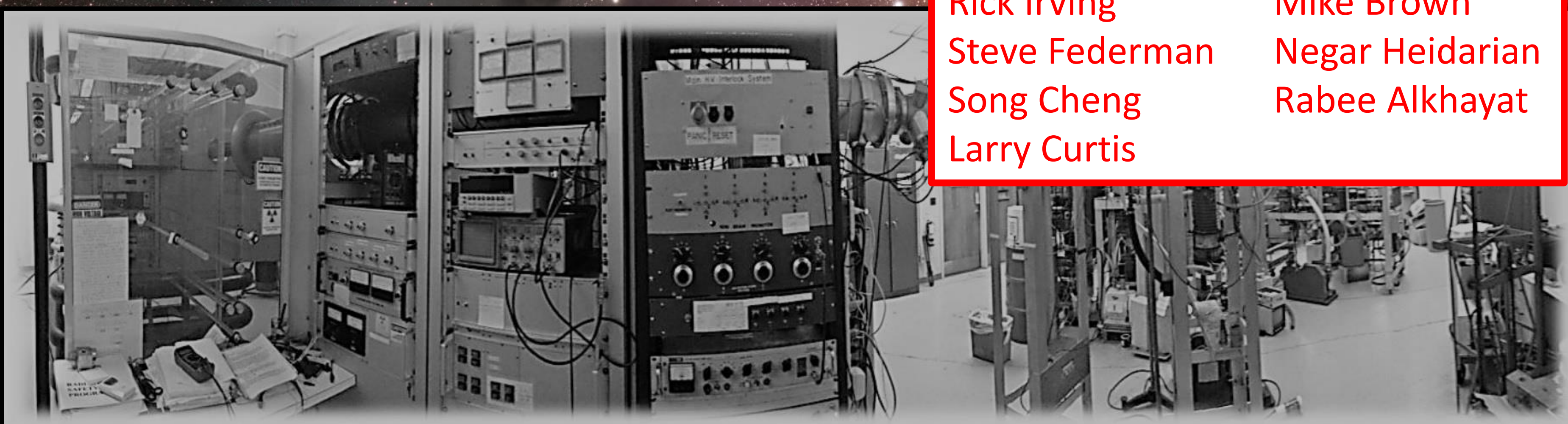

The THIA team:

Rick Irving
Steve Federman
Song Cheng
Larry Curtis
Mike Brown
Negar Heidarian
Rabee Alkhayat

Improvements in Oscillator Strengths

Lifetimes determined through analysis of decay curves.

For example, for Ge II λ1237, the lifetime of the $4s^2 4d\ ^2D_{3/2}$ level yields an oscillator strength of 0.872 ± 0.113.

Other commonly used *f*-values for Ge II λ1237:

1.23 (Biémont et al. 1998; Morton 2000; Cashman et al. 2017)
0.8756 (Morton 1991)

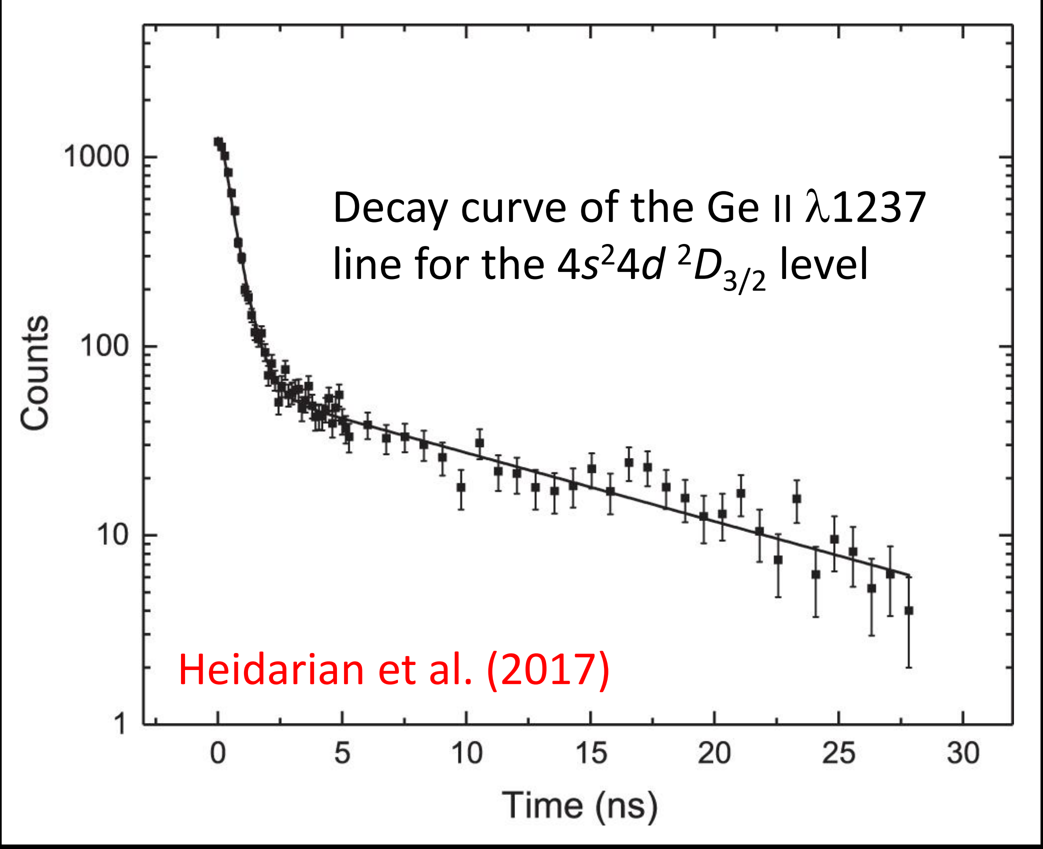

Improvements in Oscillator Strengths

Lifetimes determined through analysis of decay curves.

For example, for Ge II λ1237, the lifetime of the $4s^2 4d\ ^2D_{3/2}$ level yields an oscillator strength of 0.872 ± 0.113.

Other commonly used *f*-values for Ge II λ1237:

1.23 (Biémont et al. 1998; Morton 2000; Cashman et al. 2017)
0.8756 (Morton 1991)

a 0.15 dex increase in column density over the value adopted in Morton (2000) and Cashman et al. (2017)

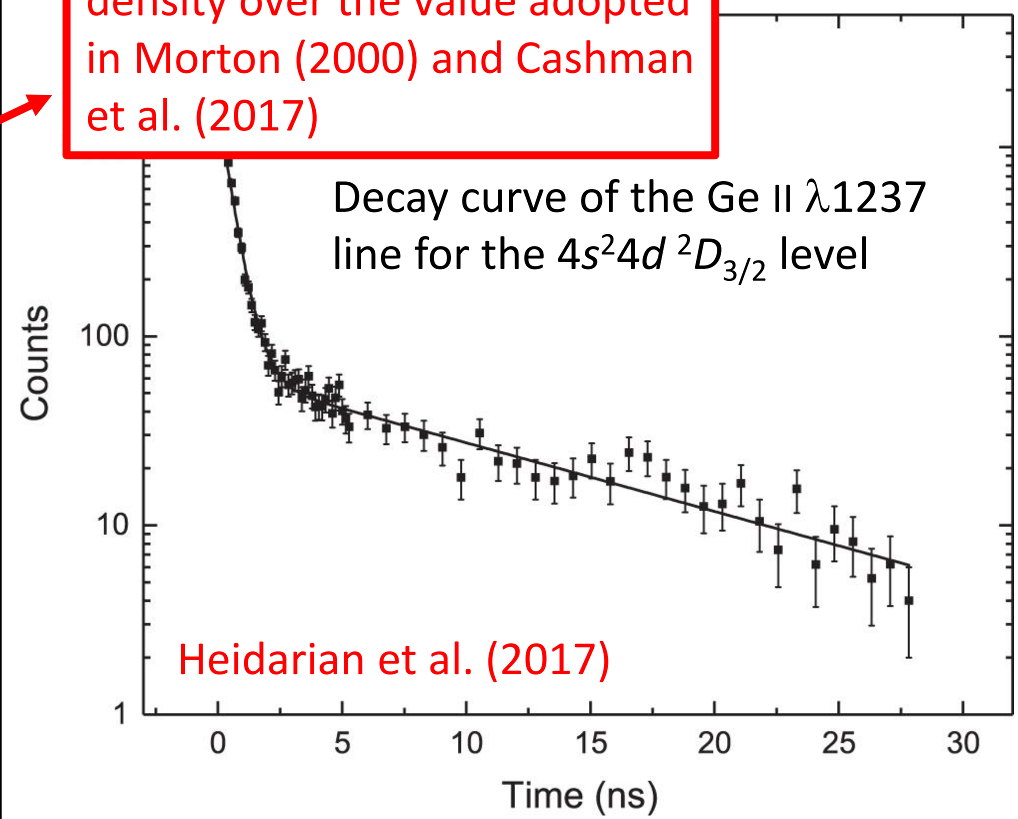

Improvements in Oscillator Strengths

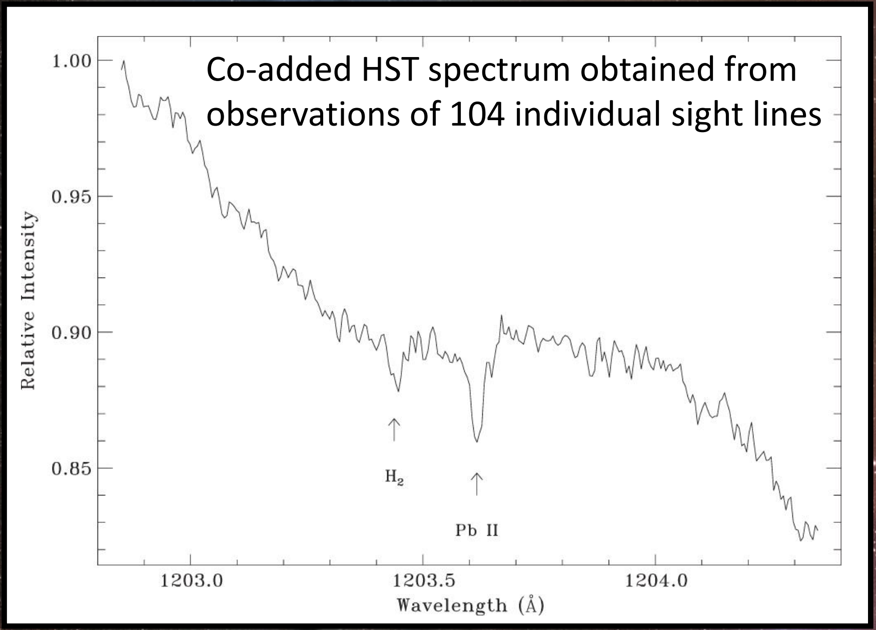

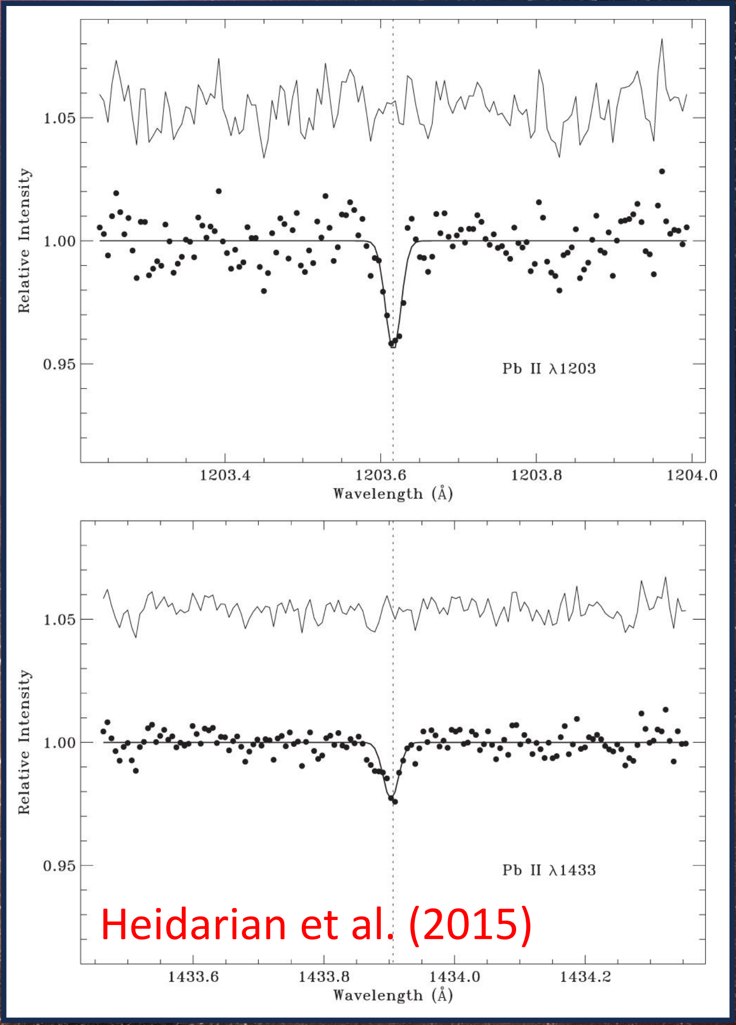

Discovered a previously undetected interstellar line of Pb II at 1203.6 Å in co-added HST spectra.

By comparing the line strength to the known Pb II λ1433 feature, we derived an empirical *f*-value ratio of $f_{1203}/f_{1433} = 2.34 \pm 0.43$.

Improvements in Oscillator Strengths

Beam-foil experiments with THIA confirm our results based on interstellar spectra.

We find oscillator strengths of 0.321 ± 0.034 for Pb II λ1433 and 0.75 ± 0.03 for Pb II λ1203.

Other commonly used *f*-values for Pb II λ1433:

0.4518 (Safronova et al. 2005; Cashman et al. 2017)
0.869 (Migdalek 1976; Morton 2000)

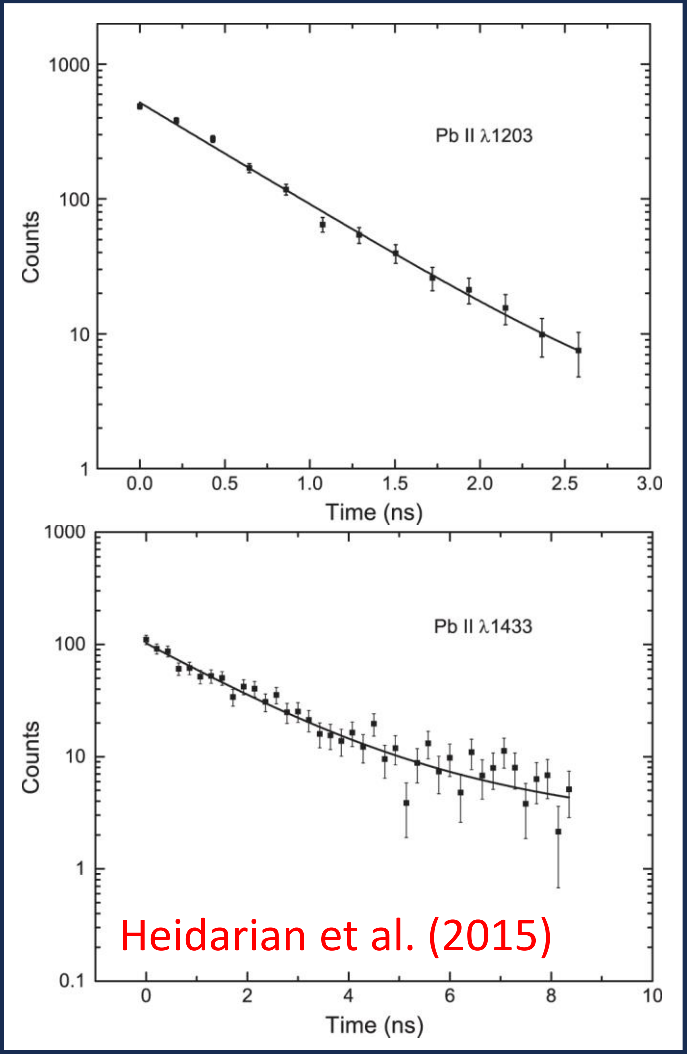

Improvements in Oscillator Strengths

Beam-foil experiments with THIA confirm our results based on interstellar spectra.

We find oscillator strengths of 0.321 ± 0.034 for Pb II λ1433 and 0.75 ± 0.03 for Pb II λ1203.

a 0.43 dex increase in column density over the value adopted in Morton (2000)

Other commonly used *f*-values for Pb II λ1433

0.4518 (Safronova et al. 2005; Cashman et al. 2017)
0.869 (Migdalek 1976; Morton 2000)

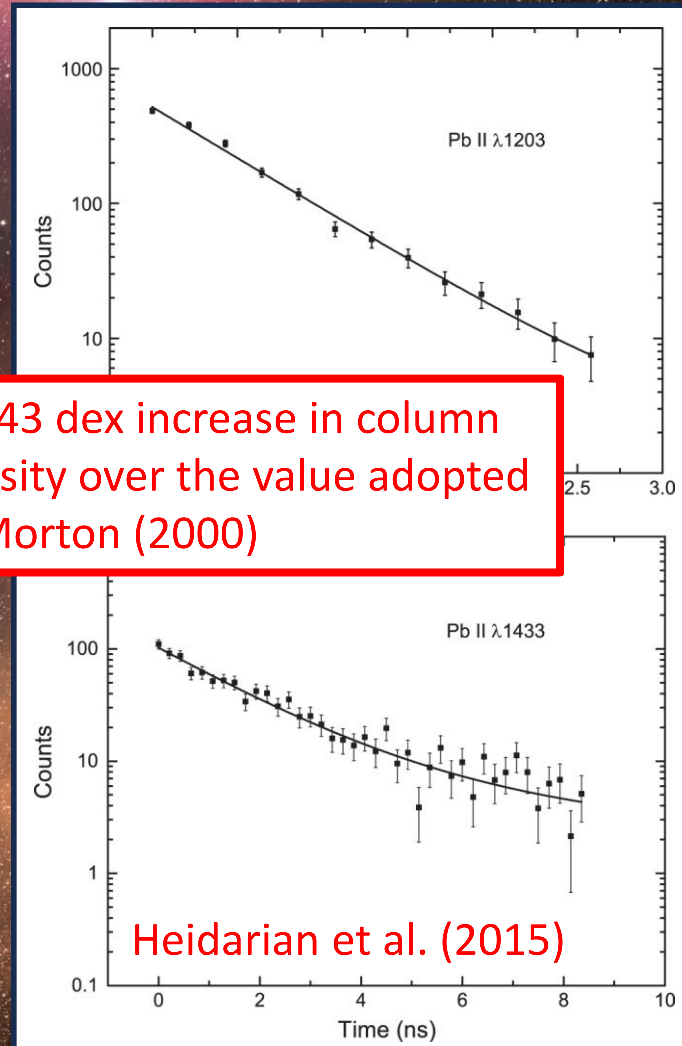

Results on Dust Depletions

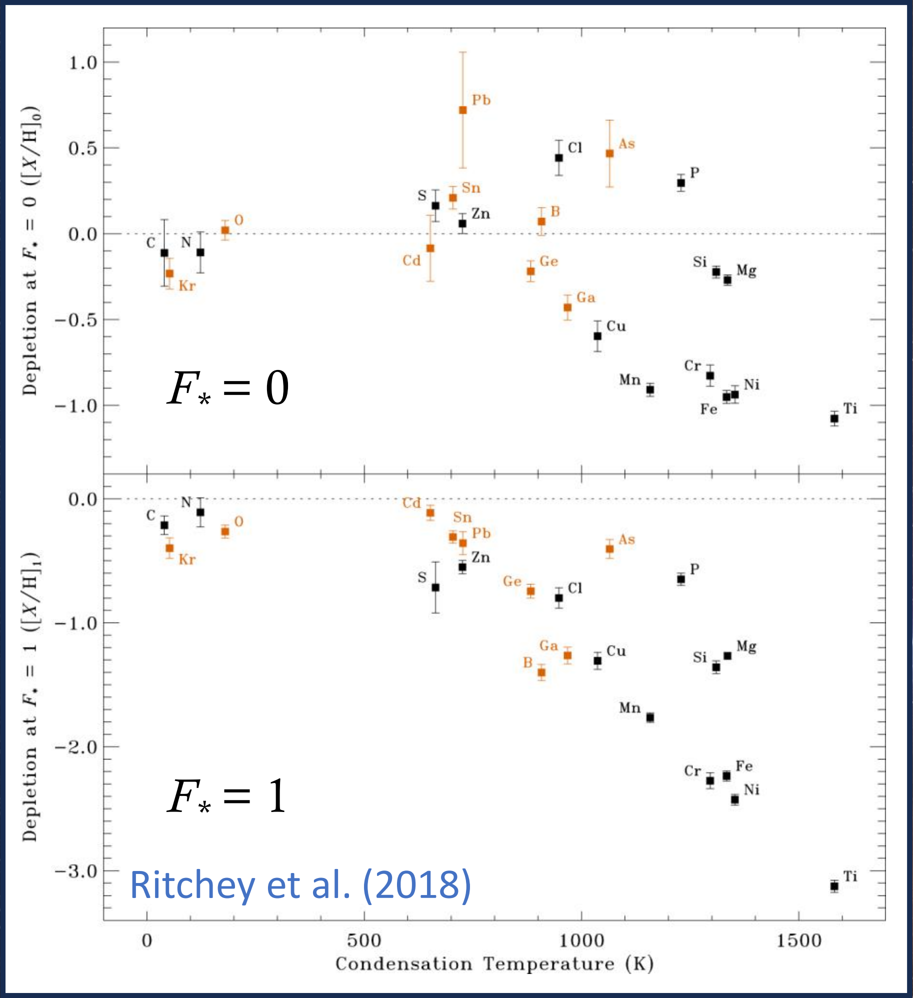

Dust depletions seen along low-depletion sight lines (with $F_* \approx 0$) likely represent the resilient cores of dust grains that emerge from evolved stars and SNe.

Depletions associated with high-depletion sight lines (with $F_* \approx 1$) result from the growth of dust grains in cold interstellar clouds.

Results on Dust Depletions

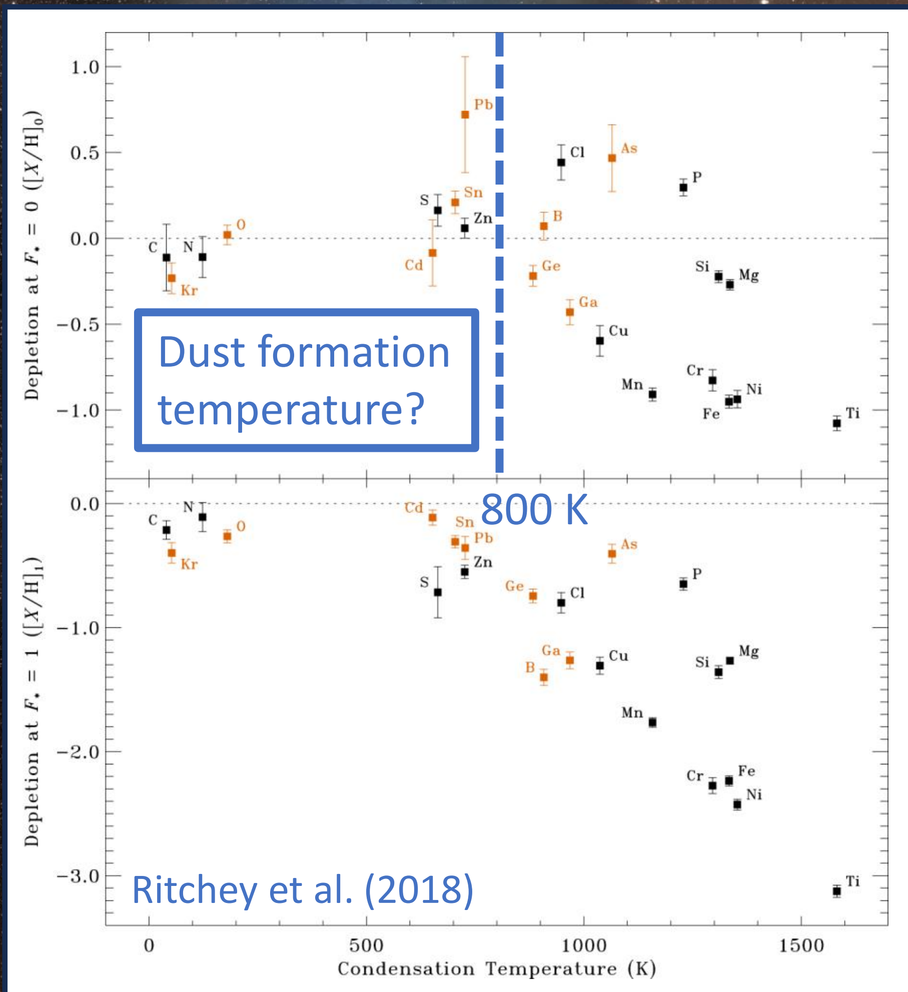

Dust depletions seen along low-depletion sight lines (with $F_* \approx 0$) likely represent the resilient cores of dust grains that emerge from evolved stars and SNe.

Depletions associated with high-depletion sight lines (with $F_* \approx 1$) result from the growth of dust grains in cold interstellar clouds.

Results on Dust Depletions

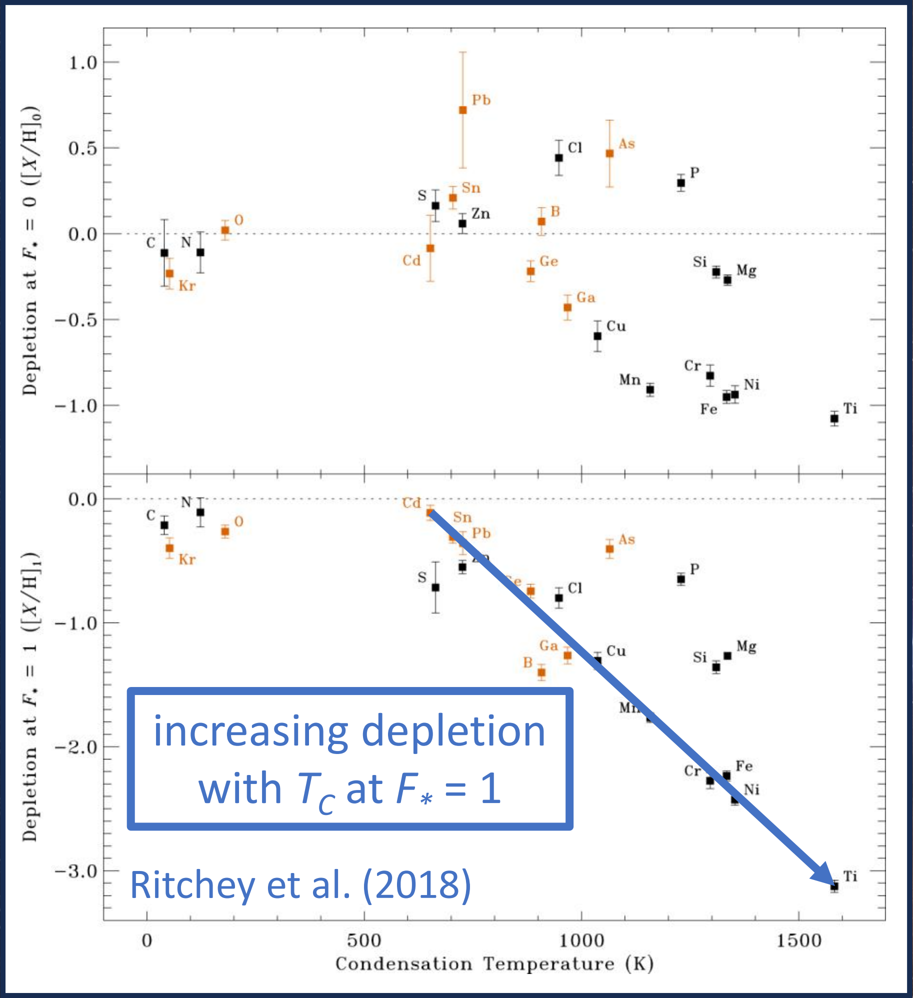

Dust depletions seen along low-depletion sight lines (with $F_* \approx 0$) likely represent the resilient cores of dust grains that emerge from evolved stars and SNe.

Depletions associated with high-depletion sight lines (with $F_* \approx 1$) result from the growth of dust grains in cold interstellar clouds.

Results on Dust Depletions

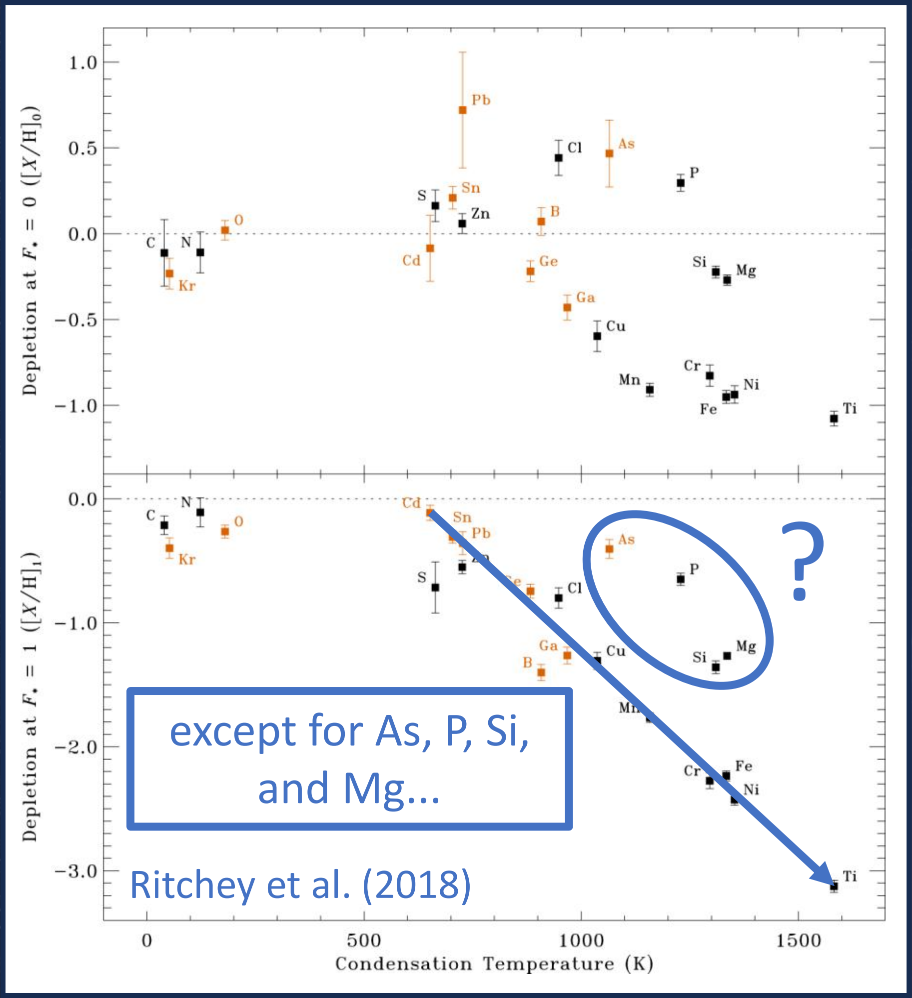

Dust depletions seen along low-depletion sight lines (with $F_* \approx 0$) likely represent the resilient cores of dust grains that emerge from evolved stars and SNe.

Depletions associated with high-depletion sight lines (with $F_* \approx 1$) result from the growth of dust grains in cold interstellar clouds.

Results on Dust Depletions

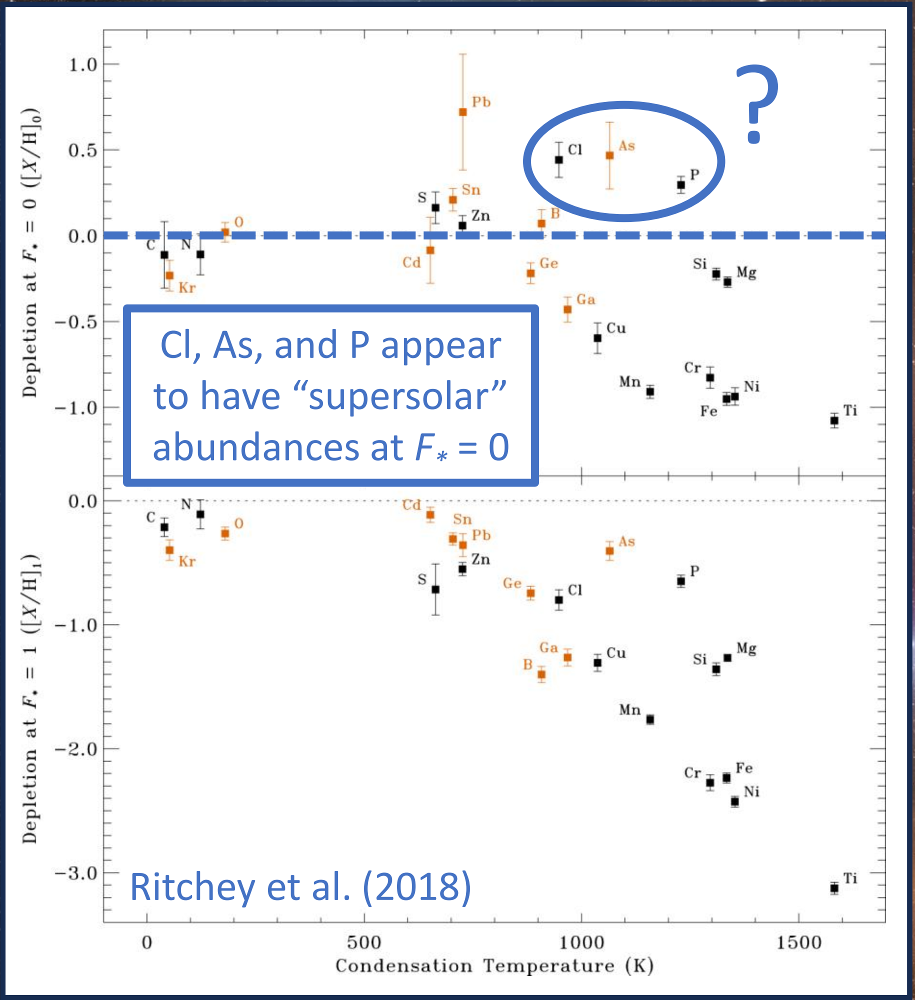

Dust depletions seen along low-depletion sight lines (with $F_* \approx 0$) likely represent the resilient cores of dust grains that emerge from evolved stars and SNe.

Depletions associated with high-depletion sight lines (with $F_* \approx 1$) result from the growth of dust grains in cold interstellar clouds.

Unusual Results for P and Cl

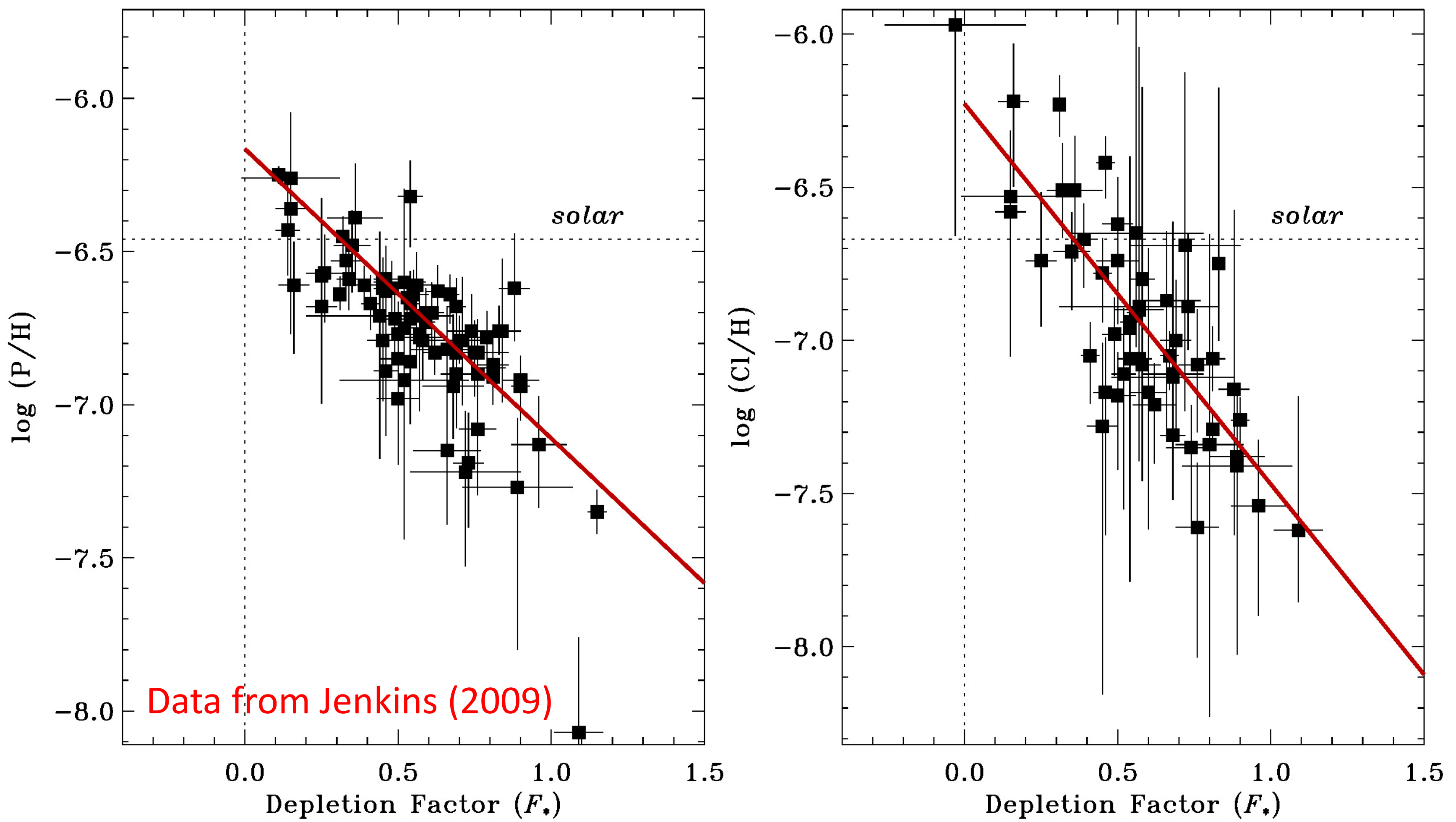

Unusual Results for P and Cl

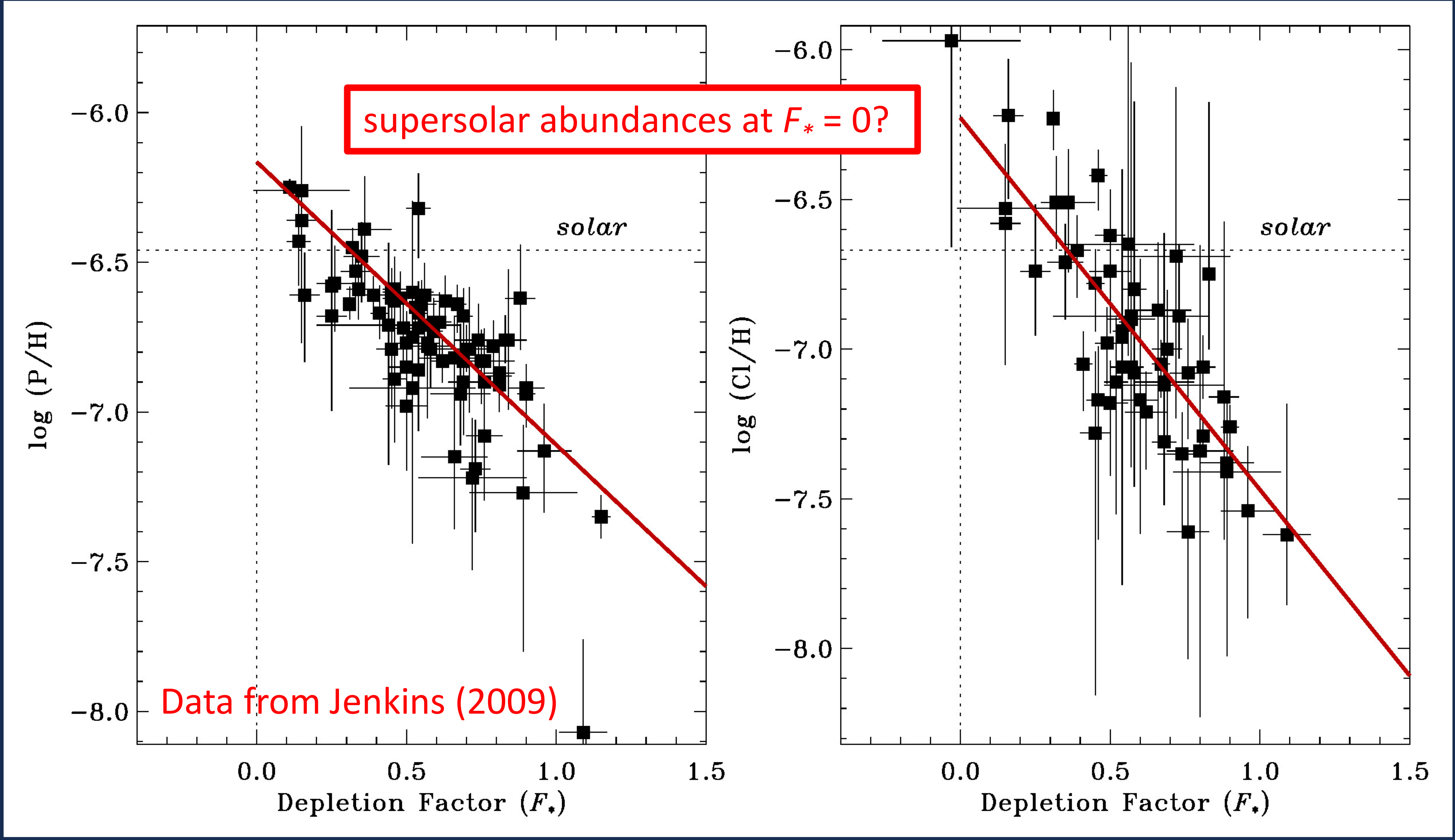

Updated *f*-values for P II and Cl I

New experimental *f*-value for P II λ1301 determined using beam foil techniques with THIA: 0.0196 ± 0.002 (Brown et al. 2018).

Other commonly used *f*-values for P II λ1301:

0.0210 (Froese Fischer et al. 2006; Cashman et al. 2017)
0.0207 (Tayal 2003)
0.0127 (Hibbert 1988; Morton 2003)
0.01725 (Livingston et al. 1975; Morton 1991)

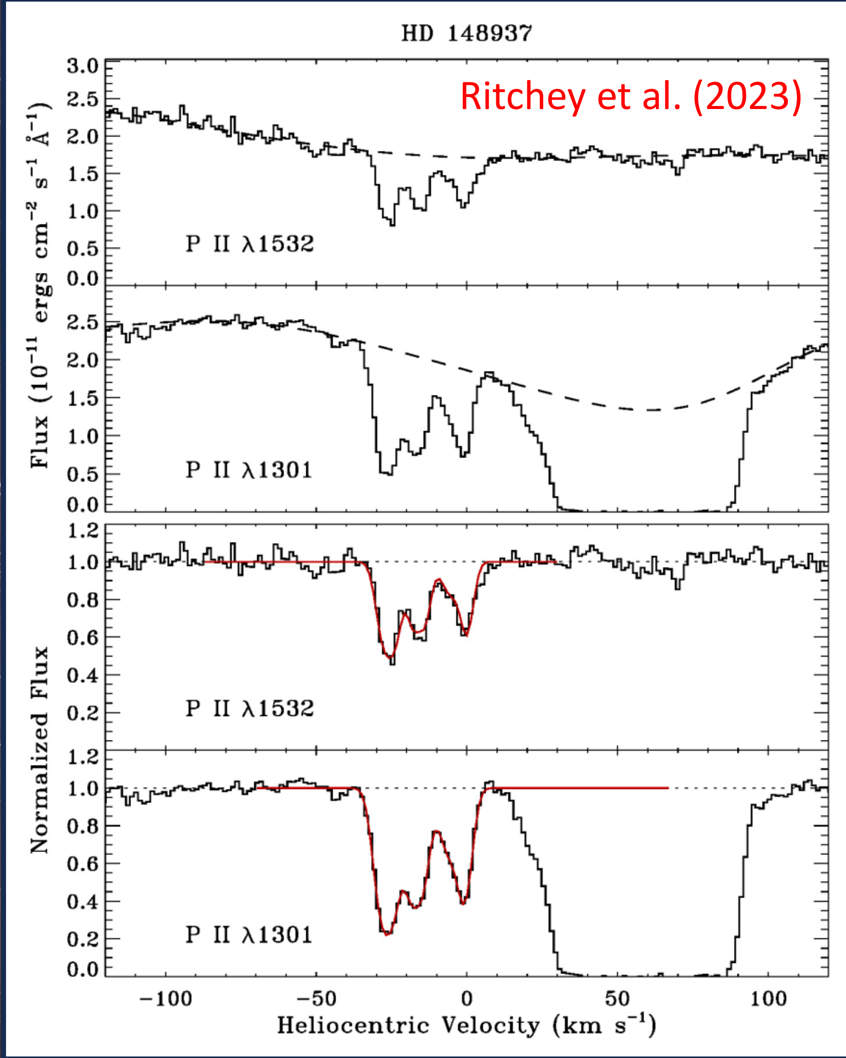

Updated *f*-values for P II and Cl I

New experimental *f*-value for P II λ1301 determined using beam foil techniques with THIA: 0.0196 ± 0.002 (Brown et al. 2018).

a decrease in column density of 0.19 dex relative to the value adopted in Morton (2003)

Other commonly used *f*-values for P II λ1301:

0.0210 (Froese Fischer et al. 2006; Cashman et al. 2017)
0.0207 (Tayal 2003)
0.0127 (Hibbert 1988; Morton 2003)
0.01725 (Livingston et al. 1975; Morton 1991)

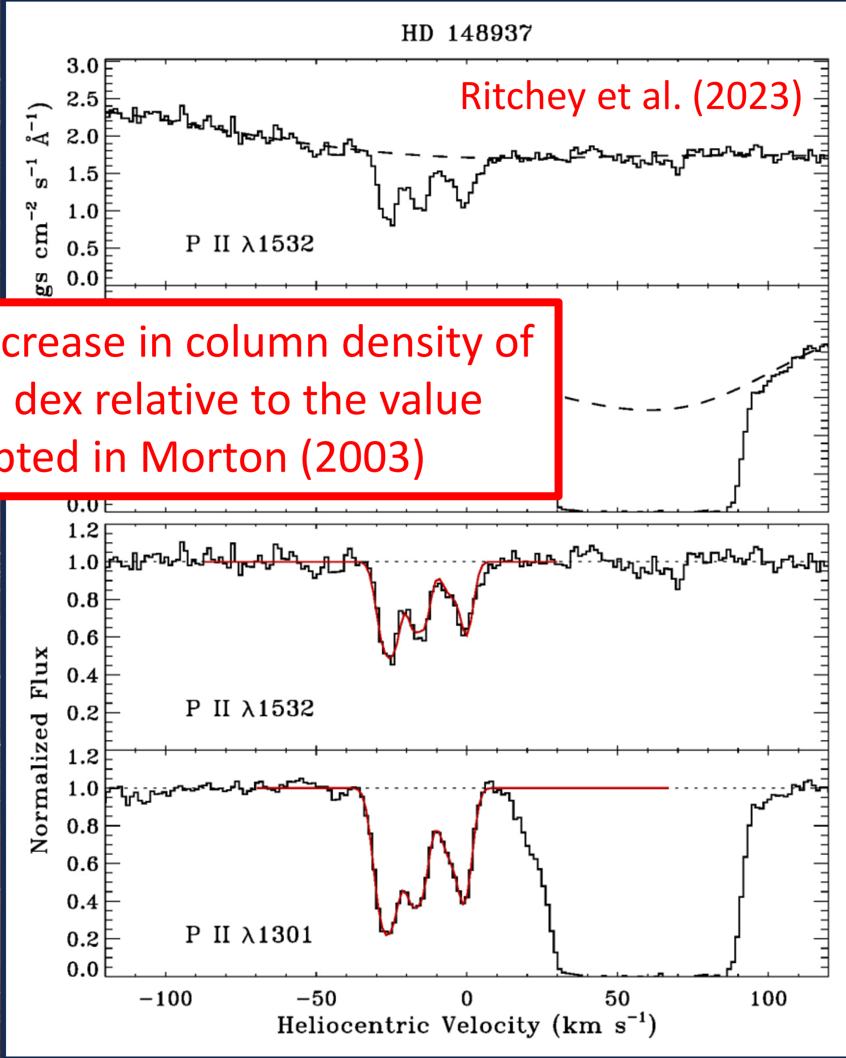

Updated *f*-values for P II and Cl I

We then derived an empirical *f*-value for P II λ1532 through profile fitting of the λ1301 and λ1532 lines in HST spectra. Our result: $f = 0.00737$.

Other commonly used *f*-values for P II λ1532:

- 0.00701 (Froese Fischer et al. 2006; Cashman et al. 2017)
- 0.00793 (Tayal 2003)
- 0.00303 (Hibbert 1988; Morton 2003)
- 0.007610 (Savage & Lawrence 1966; Morton 1991)

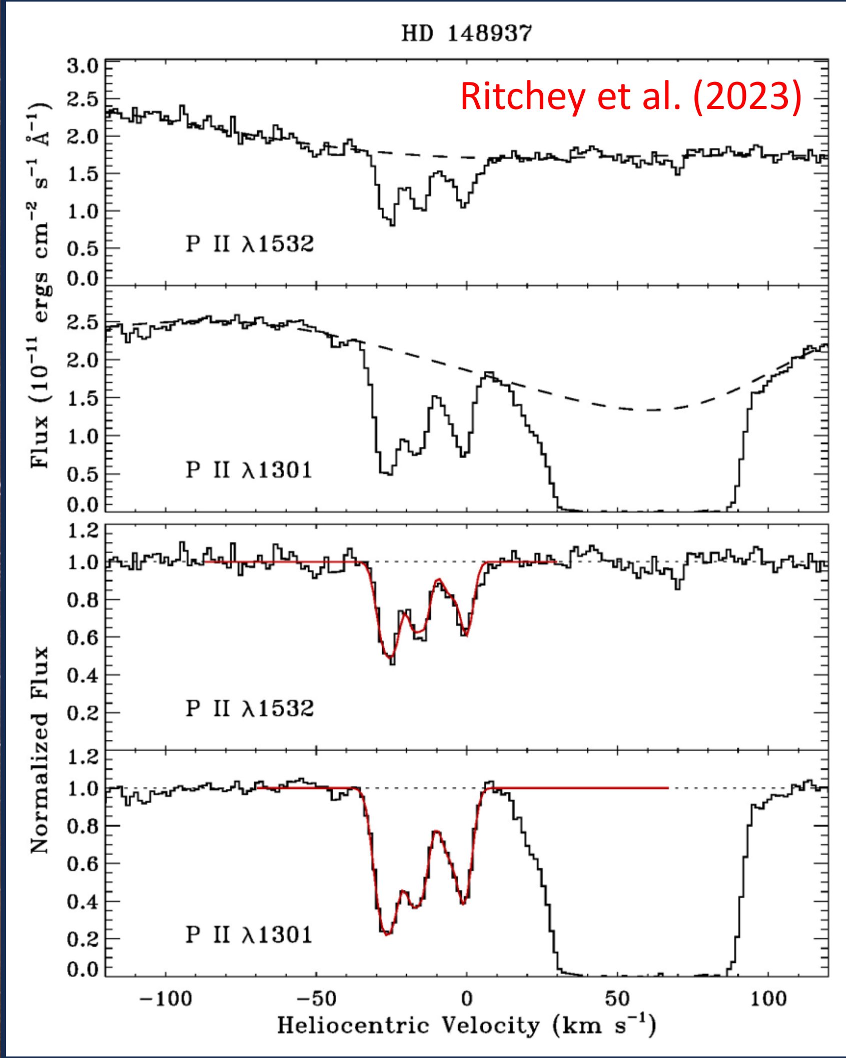

Updated *f*-values for P II and Cl I

We then derived an empirical *f*-value for P II λ1532 through profile fitting of the λ1301 and λ1532 lines in HST spectra. Our result: $f = 0.00737$.

a decrease in column density of 0.39 dex relative to the value adopted in Morton (2003)

Other commonly used *f*-values for P II λ1532:

0.00701 (Froese Fischer et al. 2006; Cashman et al. 2017)
0.00793 (Tayal 2003)
0.00303 (Hibbert 1988; Morton 2003)
0.007610 (Savage & Lawrence 1966; Morton 1991)

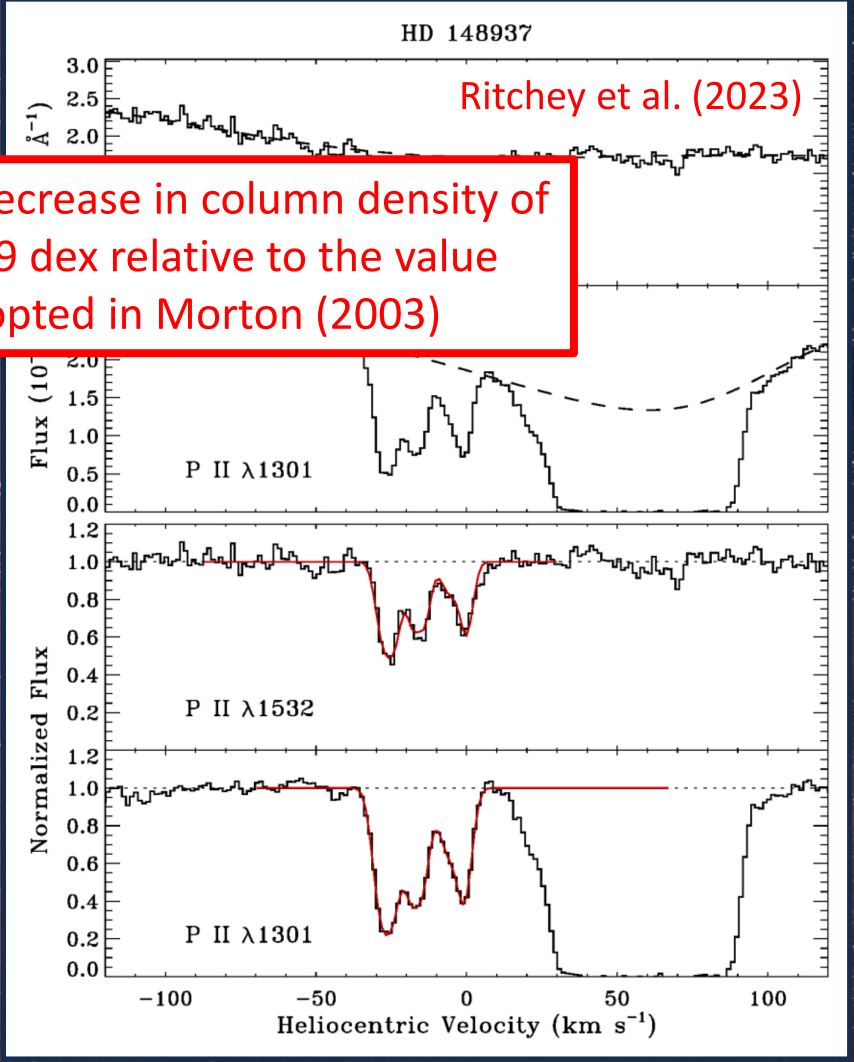

Updated *f*-values for P II and Cl I

New experimental *f*-values obtained with THIA for several UV transitions in Cl I: 0.0473 ± 0.0036 for λ1004, 0.0385 ± 0.0011 for λ1094 (Alkhayat et al. 2019).

Other *f*-values for Cl I λ1004:

0.04427 (Oliver & Hibbert 2013; Cashman et al. 2017)
0.0514 (Sonnentrucker et al. 2006)
0.1577 (Kurucz & Peytremann 1975; Morton 1991)

Other *f*-values for Cl I λ1094:

0.03224 (Oliver & Hibbert 2013)
0.0396 (Sonnentrucker et al. 2006)
0.0166 (Biémont et al. 1994; Morton 2003)
0.0011 (Ojha & Hibbert 1990; Morton 1991)

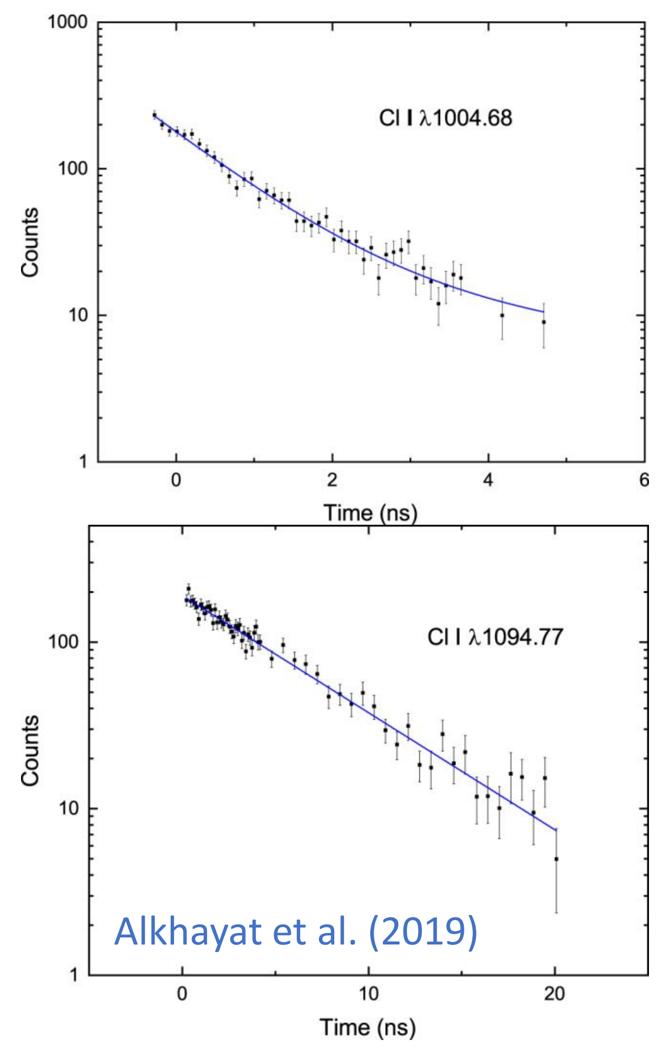

Updated *f*-values for P II and Cl I

New experimental *f*-values obtained with THIA for several UV transitions in Cl I: 0.0473 ± 0.0036 for λ1004, 0.0385 ± 0.0011 for λ1094 (Alkhayat et al. 2019).

Other *f*-values for Cl I λ1004:

0.04427 (Oliver & Hibbert 2013; Cashman et al. 2017)

0.0514 (Sonnentrucker et al. 2006)

0.1577 (Kurucz & Peytremann 1975; Morton 1991)

Other *f*-values for Cl I λ1094:

0.03224 (Oliver & Hibbert 2013)

0.0396 (Sonnentrucker et al. 2006)

0.0166 (Biémont et al. 1994; Morton 2003)

0.0011 (Ojha & Hibbert 1990; Morton 1991)

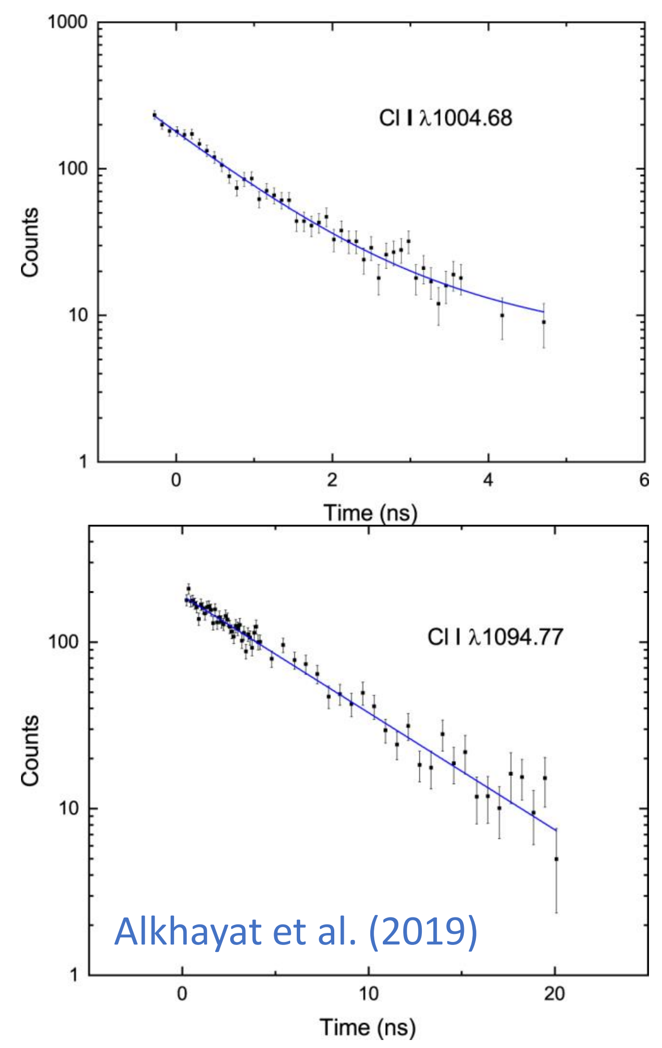

Updated *f*-values for P II and Cl I

New experimental *f*-values obtained with THIA for several UV transitions in Cl I: 0.0473 ± 0.0036 for λ1004, 0.0385 ± 0.0011 for λ1094 (Alkhayat et al. 2019).

Other *f*-values for Cl I λ1004:

0.04427 (Oliver & Hibbert 2013; Cashman et al. 2017)
0.0514 (Sonnentrucker et al. 2006)
0.1577 (Kurucz & Peytremann 1975; Morton 1991)

Other *f*-values for Cl I λ1094:

0.03224 (Oliver & Hibbert 2013)
0.0396 (Sonnentrucker et al. 2006)
0.0166 (Biémont et al. 1994; Morton 2003)
0.0011 (Ojha & Hibbert 1990; Morton 1991)

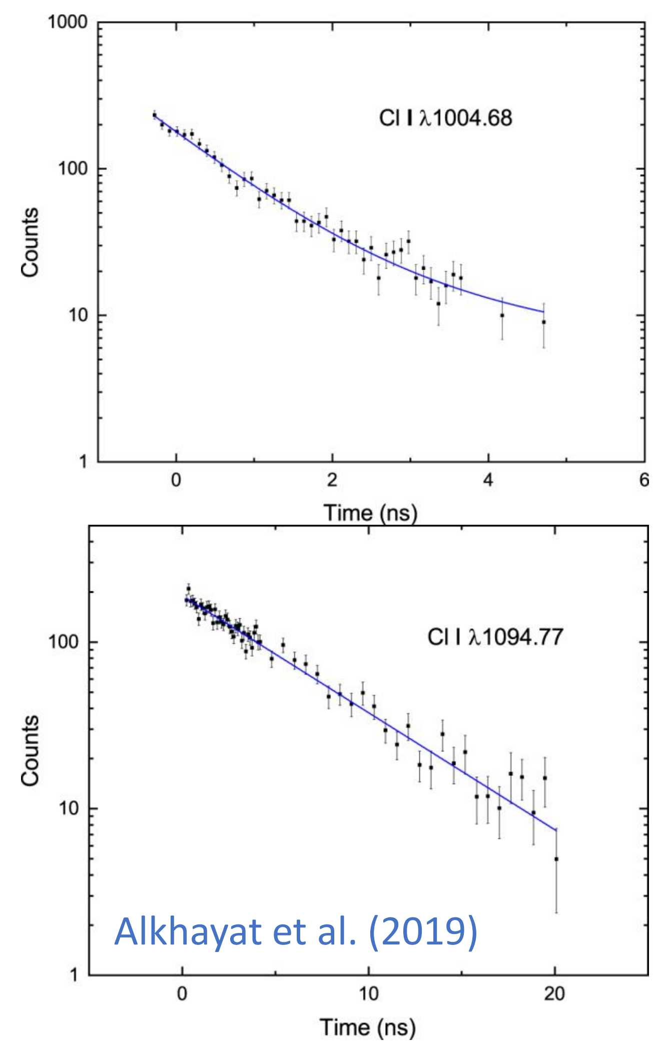

Updated Results for P and Cl

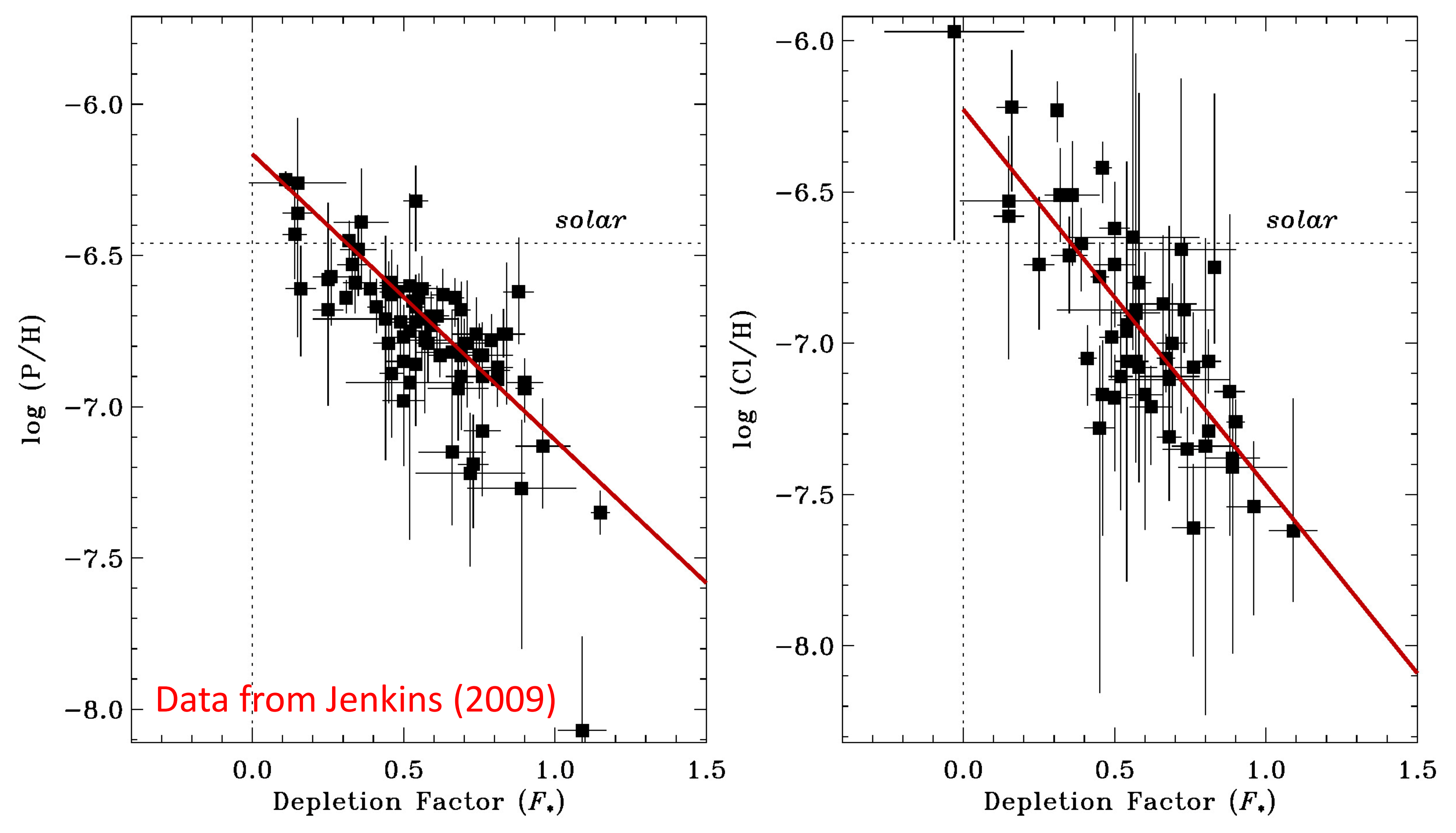

Updated Results for P and Cl

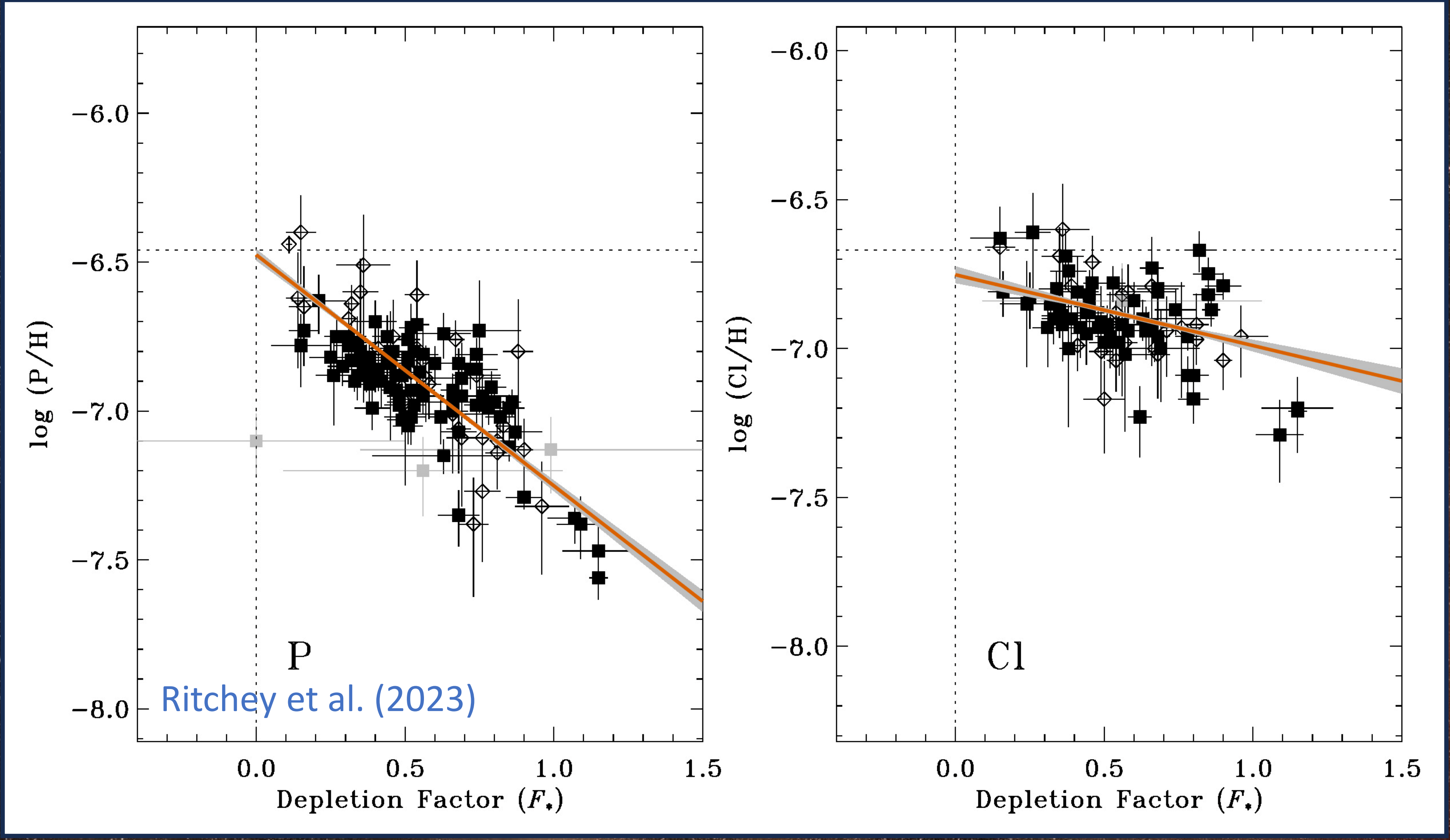

New Experimental *f*-values Needed

Transitions in need of experimental confirmation of *f*-value:

	M91	M03	C17
Mn II λ1197	0.157	0.217	0.148
Mn II λ1199	0.106	0.169	0.116
Mn II λ1201	0.088	0.121	0.083

	M91	JT06	C17	BB19
Ni II λ1317	0.1458	0.0571	0.0818	0.0596
Ni II λ1370	0.1309	0.0588	0.0811	0.0616

	M00
As II λ1263	0.259

New Experimental *f*-values Needed

Transitions in need of experimental confirmation of *f*-value:

	M91	M03	C17
Mn II λ1197	0.157	0.217	0.148
Mn II λ1199	0.106	0.169	0.116
Mn II λ1201	0.088	0.121	0.083

interstellar absorption (Lugger et al. 1982)

	M91	JT06	C17	BB19
Ni II λ1317	0.1458	0.0571	0.0818	0.0596
Ni II λ1370	0.1309	0.0588	0.0811	0.0616

	M00
As II λ1263	0.259

New Experimental *f*-values Needed

Transitions in need of experimental confirmation of *f*-value:

	M91	M03	C17	
Mn II λ1197	0.157	0.217	0.148	
Mn II λ1199	0.106	0.169	0.116	
Mn II λ1201	0.088	0.121	0.083	
		theory (Kurucz 1998)		
	M91	JT06	C17	BB19
Ni II λ1317	0.1458	0.0571	0.0818	0.0596
Ni II λ1370	0.1309	0.0588	0.0811	0.0616
	M00			
As II λ1263	0.259			

New Experimental *f*-values Needed

Transitions in need of experimental confirmation of *f*-value:

	M91	M03	C17
Mn II λ1197	0.157	0.217	0.148
Mn II λ1199	0.106	0.169	0.116
Mn II λ1201	0.088	0.121	0.083

theory (Toner & Hibbert 2005)

	M91	JT06	C17	BB19
Ni II λ1317	0.1458	0.0571	0.0818	0.0596
Ni II λ1370	0.1309	0.0588	0.0811	0.0616

	M00
As II λ1263	0.259

New Experimental *f*-values Needed

Transitions in need of experimental confirmation of *f*-value:

	M91	M03	C17
Mn II λ1197	0.157	0.217	0.148
Mn II λ1199	0.106	0.169	0.116
Mn II λ1201	0.088	0.121	0.083

	M91	JT06	C17	BB19
Ni II λ1317	0.1458	0.0571	0.0818	0.0596
Ni II λ1370	0.1309	0.0588	0.0811	0.0616

theory (Kurucz 1989)

	M00
As II λ1263	0.259

New Experimental *f*-values Needed

Transitions in need of experimental confirmation of *f*-value:

	M91	M03	C17
Mn II λ1197	0.157	0.217	0.148
Mn II λ1199	0.106	0.169	0.116
Mn II λ1201	0.088	0.121	0.083

	M91	JT06	C17	BB19
Ni II λ1317	0.1458	0.0571	0.0818	0.0596
Ni II λ1370	0.1309	0.0588	0.0811	0.0616

interstellar absorption (Jenkins & Tripp 2006)

	M00
As II λ1263	0.259

New Experimental *f*-values Needed

Transitions in need of experimental confirmation of *f*-value:

	M91	M03	C17
Mn II λ1197	0.157	0.217	0.148
Mn II λ1199	0.106	0.169	0.116
Mn II λ1201	0.088	0.121	0.083

	M91	JT06	C17	BB19
Ni II λ1317	0.1458	0.0571	0.0818	0.0596
Ni II λ1370	0.1309	0.0588	0.0811	0.0616

theory (Cassidy et al. 2016)

	M00
As II λ1263	0.259

New Experimental *f*-values Needed

Transitions in need of experimental confirmation of *f*-value:

	M91	M03	C17
Mn II λ1197	0.157	0.217	0.148
Mn II λ1199	0.106	0.169	0.116
Mn II λ1201	0.088	0.121	0.083

	M91	JT06	C17	BB19
Ni II λ1317	0.1458	0.0571	0.0818	0.0596
Ni II λ1370	0.1309	0.0588	0.0811	0.0616

quasar absorption lines (Boissé & Bergeron 2019)

	M00
As II λ1263	0.259

New Experimental *f*-values Needed

Transitions in need of experimental confirmation of *f*-value:

	M91	M03	C17
Mn II λ1197	0.157	0.217	0.148
Mn II λ1199	0.106	0.169	0.116
Mn II λ1201	0.088	0.121	0.083

	M91	JT06	C17	BB19
Ni II λ1317	0.1458	0.0571	0.0818	0.0596
Ni II λ1370	0.1309	0.0588	0.0811	0.0616

	M00
As II λ1263	0.259

theory (Biémont et al. 1998)

Enhanced Arsenic Abundance?

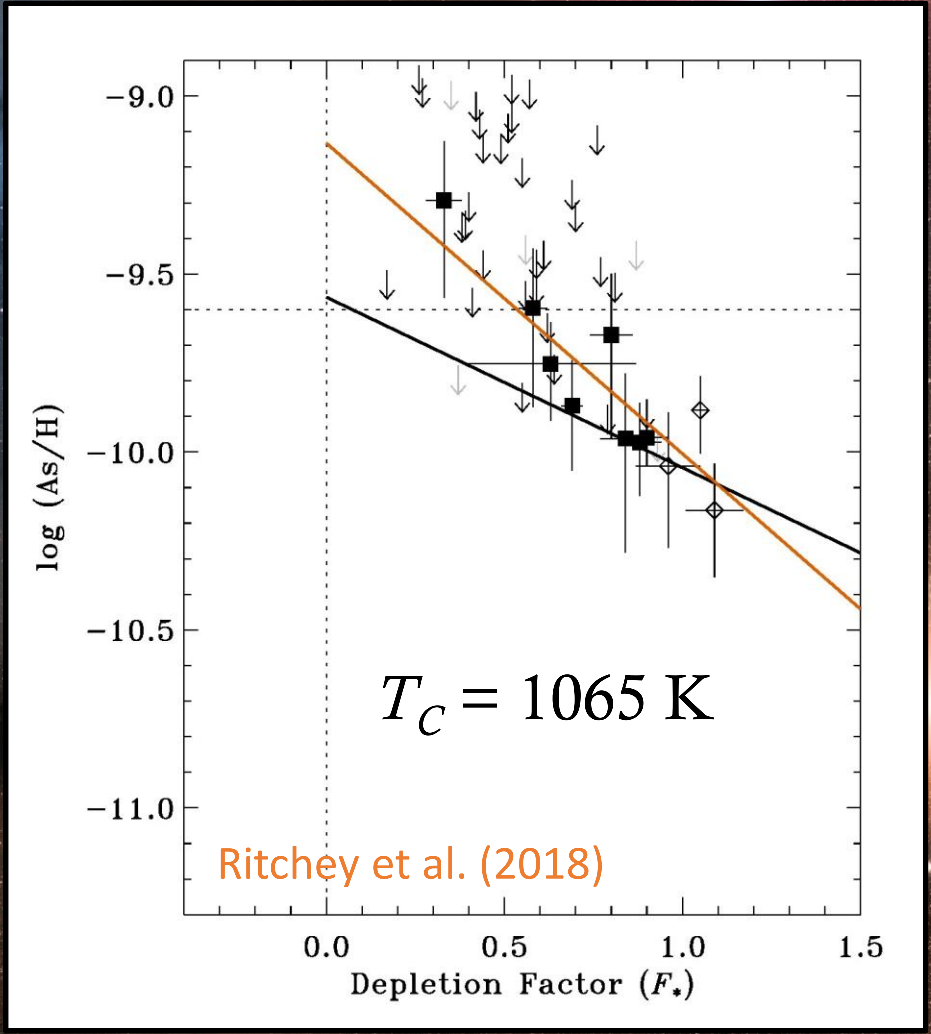

Summary/Conclusions

- Accurate oscillator strengths are crucial for understanding interstellar gas-phase abundances and dust-grain depletions
- Over the past several decades, the THIA group at the University of Toledo has provided secure experimental *f*-values (from lifetime measurements using beam-foil techniques) for commonly observed transitions in P II, Cl I, Cl II, Cu II, Ge II, Sn II, and Pb II.
- These results have improved our understanding of the gas-phase abundances of neutron-capture elements and have clarified the trends exhibited by the depletions of the elements onto interstellar dust grains.
- New experimental *f*-values are needed, especially for Mn II, Ni II, and As II.